Contrib Mineral Petrol
DOI 10.1007/s00410-009-0482-6

ORIGINAL PAPER

Construction of the granitoid crust of an island arc. Part II: a quantitative petrogenetic model

Oliver E. Jagoutz

Received: 25 March 2009 / Accepted: 30 December 2009

Abstract Results of simple model calculations that integrate cumulate compositions from the Kohistan arc terrain are presented in order to develop a consistent petrogenetic model to explain the Kohistan island arc granitoids. The model allows a quantitative approximation of the possible relative roles of fractional crystallization and assimilation to explain the silica-rich upper crust composition of oceanic arcs. Depending in detail on the parental magma composition hydrous moderate-to-high pressure fractional crystallization in the lower crust/upper mantle is an adequate upper continental crust forming mechanism in terms of volume and compositions. Accordingly, assimilation and partial melting in the lower crust is not per se a necessary process to explain island arc granitoids. However, deriving few percent of melts using low degree of dehydration melting is a crucial process to produce volumetrically important amounts of upper continental crust from silica-poorer parental magmas. Even though the model can explain the silica-rich upper crustal composition of the Kohistan, the fractionation model does not predict the accepted composition of the bulk continental crust. This finding supports the idea that additional crustal refining mechanism (e.g., delamination of lower crustal rocks) and/or non-cogenetic magmatic process were critical to create the bulk continental crust composition.

Keywords Continental crust · Granitoid · Crystal fractionation · Partial melting · Subduction zone

Communicated by T. L. Grove.

O. E. Jagoutz (✉)
Department of Earth, Atmospheric, and Planetary Sciences, Massachusetts Institute of Technology, Cambridge, USA
e-mail: jagoutz@mit.edu

Introduction

Based on trace element similarities, it is widely accepted that the majority of the continental crust is formed in subduction zones (Rudnick 1995), also referred to as the "andesite model" (Taylor 1977; Taylor and Mclennan 1981; Mclennan and Taylor 1982). A major problem associated with this model assumption is that the mass flux out of the mantle in subduction zones is thought to be generally basaltic (SiO_2 <52 wt%), whereas the accepted bulk continental crust composition is andesitic (SiO_2 ~60 wt%). As the lower crust is basaltic in composition, the silica-rich composition of the bulk continental crust is the result of silica-rich upper crustal granitoids (Rudnick and Gao 2003). Accordingly, insight into the formation mechanisms of the granitoids in subduction zone settings will improve our understanding of the silica-rich nature of the continental crust.

Generally, processes in the lower continental crust and the upper mantle are considered crucial to the formation of upper continental crust. Specifically, moderate-to-high pressure fractional crystallization, partial melting, and foundering of high-density cumulates/restites have the potential to produce upper continental crust and thereby strongly modify the lower and bulk continental crust (e.g., Sisson et al. 2005; Müntener and Ulmer 2006). However, our detailed knowledge of these processes and their relative importance is extremely limited, and the lower crust/upper mantle remains the "black box" of crust formation. Our understanding of the importance of the role of the lower continental crust for upper crust formation is additionally hampered by the fact that the preserved lower continental crust is not complement to the upper continental crust. The preserved lower continental crust, with only a minor positive europium anomaly and the generally near

Published online: 17 February 2010

primitive arc basalt incompatible element concentrations, is inadequate to complement the upper continental crust to arrive at a mantle-derived melt composition (e.g., Hawkesworth and Kemp 2006).

This paper, the second of two papers, aims to integrate field, petrographic, and geochronological observations from the Kohistan arc, presented in the first paper (Jagoutz et al. 2009), into a petrogenetic model to explain the composition of the Kohistan arc granitoids. In the first paper it was shown that the granitoids in Kohistan are temporally unrelated to the intrusion of large mafic bodies and that granitoids are formed by a continuous steady state process. In this paper, I will focus on the relative role of two important end member hypotheses put forward for granitoid formation in arcs, which are conflicting: (1) magmatic differentiation from a mafic magma in a single stage process (Bowen 1928; Tuttle and Bowen 1958); (2) partial melting of the basaltic (amphibolitic) lower crust triggered by magma addition invoking a multistage scenario (e.g., White and Chapell 1983; Pitcher 1997).

The fact that the relative importance of fractionation and partial melting to generate the upper crust remains contentious even after decades of research reflects the difficulty in distinguishing these two end-member processes. The volatile content is crucial for controlling the effectiveness in producing evolved melt compositions (Jagoutz et al. 2009). In a near-dry system, where the volatile content is sufficiently low that all can be retained in the minerals, partial melting and crystal fractionation yield indistinguishable melt-restite/cumulate relations under equilibrium conditions. For arcs, partial melting will be less productive of evolved melts because rocks typically can retain no more than $\sim$2 wt% H_2O, whereas primitive arc magmas can have high initial water content (up to 10 wt%, Grove et al. 2002, 2003). In continental arcs the importance of partial melting/assimilation of old, isotopic-evolved continental basement can be monitored through radiogenic isotopic data (e.g., Sr, Nd Pb), which is thought to indicate significant involvement of pre-existing crust into arc magmas (e.g., Hildreth and Moorbath 1988). Yet, it has been argued that oxygen isotopes imply a significant ($\geq$80%) mantle contribution to continental arc granitoids (Kemp et al. 2007). A certain level of ambiguity exists concerning the origin of a "crustal isotopic signature" in arcs (e.g., Gill 1981). It is generally accepted that a hydrous so-called "slab-derived component" (Grove et al. 2002; Jagoutz et al. 2007) expelled from the subducted slab due to dehydration or partial melting reactions triggers flux melting in the mantle wedge producing arc magmas (McCulloch and Gamble 1991). Subducted sediments are thought to contribute to arc magmatism by these processes (e.g., Morris et al. 1990) and have comparable isotopic signatures as the upper continental plate in continental arcs (e.g., Plank 2005). Due to this similarity in isotopic composition, it is difficult to distinguish the relative contribution of subducted sediments versus intra continental assimilation processes.

In oceanic arcs where old isotopically evolved continental basement is absent and subducted continental sediments can be minor, the role of assimilation is even less clear. Oxygen isotopes indicate a limited contribution of a "crustal component" into intra-oceanic arc magmas (Eiler et al. 2000, 2007), but qualitative indicators of assimilation such as xenoliths of plutonic rocks and the presence of older inherited zircons in younger arc granitoids indeed document intra crustal assimilation processes (Jagoutz et al. 2009).

An additional important constraint on the role of partial melting and assimilation comes from heat budget consideration: In continental arcs, partial melting might occur due to muscovite, biotite, and amphibole dehydration reactions, which occurs at temperatures of 665 to 920°C between 0.5 and 1.0 GPa (Clemens and Vielzeuf 1987).

In oceanic arcs, dehydration melting is thought to occur dominantly due to the breakdown of amphibole present in hydrated mafic rocks, which occurs at significantly higher temperatures (900–920°C at 0.5–1.0 GPa and at $\sim$700°C at 1.0–2.5 GPa water saturated, Clemens and Vielzeuf 1987; Vielzeuf and Schmidt 2001). Even though partial melting mechanisms have received considerable attention to explain geochemical trace element data of upper crustal granitoids, the heat source triggering this reaction is poorly constrained and often the source of speculation. The classical model invokes underplating of large basaltic sills as a heat source (Huppert and Sparks 1988). More recent numerical models, however, predict that such large sills are not very efficient in instigating widespread lower crustal melting. Intrusions of sequences of spatially and temporally overlapping dykes might produce more voluminous melts, but the general conclusion is that evolved melts are generally produced due to differentiation, not melting (Dufek and Bergantz 2005; Annen et al. 2006).

Alternatively, the "steady-state" geotherm in arcs could be hot enough to intersect the, e.g., amphibole solidus at lower crustal depth thereby triggering partial melting without invoking additional "external" heat sources (e.g., underplating). Estimates for "steady-state" geotherms in arcs are difficult to constraint and vary widely (Kelemen et al. 2003b; Dufek and Bergantz 2005; Hacker et al. 2008). Depending in detail on the data source used, the inferred geotherm is either hot and intersects the amphibole solidus at rather shallow levels sufficient to melt the lower crust of typical oceanic arcs (i.e., 20–25 km, Kelemen et al. 2003b), or it is significantly colder and the intersection occurs significantly deeper in the crust making it an effective crust forming process only for overthickened

continental arcs (>50 km, Dufek and Bergantz 2005). Pressure and temperature estimates from the lower crust of the Kohistan and the Talkeetna yield temperatures of 800–1,000°C at pressure of 1–1.5 GPa indicating a geotherm between these two estimates (Ringuette et al. 1999; Yoshino and Okudaira 2004; Hacker et al. 2008). It is unclear whether these *P*, *T* estimates record peak metamorphic conditions or the lower crust has been hotter while the arcs were active. However, these estimates agree well with the general dataset of crustal granulites terrains (Harley 1989).

In summary, partial melting of the lower crust becomes increasingly important with thicker crust as in continental arcs in accordance with the geochemical evidence. Indeed, certain trace element signatures in continental arc lava suites have been used to infer the importance of intra crustal assimilation to produce silica-rich melts. In some arc magmatic suites, concentration of one or more incompatible elements fail to increase commensurate with silica enrichment [e.g., Zr, Nb at Mount Jefferson, Cascades (Conrey et al. 2001), K_2O at Mount St. Helens (Smith and Leeman 1987)]. Similarly, K/Rb commonly decreases in compositions thought to be too primitive to have saturated in a K-rich mineral (Hildreth and Moorbath 1988). In thinner oceanic arcs, in the absence of a significant heat source, volumetrically important amounts of partial melts in the lower arc crust are difficult to produce. However, silica-rich granitoids are exposed in oceanic arcs (e.g., Aleutian, New Britain, Perfit et al. 1980; Whalen 1985; Kay et al. 1990) and are inferred as volumetrically important units based on seismic velocities (e.g., Izu Bonin, Suyehiro et al. 1996; Kodaira et al. 2007) indicating that thick crust is not a necessary requisite for granitoid formation. In the absence of a thick crust or a hot geotherm, the alternative mechanism to partial melting, moderate-to-high pressure hydrous fractional crystallization, can produce volumetrically important evolved magmatic products without the need for an external heat source (e.g., Sisson et al. 2005). In general, this mechanism might provide the "easiest" explanation to produce upper continental crust, as many subduction zone magmas are hydrous and fractional crystallization does not need an external heat source to produce granitoids. Depending on the initial parental magma composition the final silica-rich fractionation products might, however, be volumetrically insufficient to explain the volumetrically significant upper continental crust.

In the light of these arguments, I present a simple major and trace element model that integrates actual cumulate compositions from the Kohistan terrain, to develop a consistent petrogenetic model for the Kohistan granitoids. I explore whether fractionation can yield oceanic arc granitoid compositions from primitive, mantle-derived melts using cumulate whole rock compositions of the Kohistan lower crust. The aim is to elucidate the relative importance of assimilation or partial melting versus fractional crystallization to produce the silica-rich derivative rocks.

As I will show, the combination of hydrous fractional crystallization and limited assimilation at lower crustal levels is very successful combination to produce upper crustal granitoids in oceanic arcs.

Geological setting

The Kohistan arc in NW Pakistan (Fig. 1) is separated from the Karakoram margin of Eurasia, to the north, by the Karakoram-Kohistan Suture Zone and from the Indian Plate, to the south, by the Indus Suture Zone. The Kohistan is generally regarded as a fossil Jurassic/Cretaceous island arc that was wedged between the Indian and Asian plates during collision (Tahirkheli et al. 1979; Bard 1983). The intraoceanic arc originated above a north-dipping subduction zone somewhere in the equatorial area of the Tethys Ocean, possibly in the vicinity of the Eurasian continent (Coward et al. 1987; Khan et al. 1993; Bignold and Treloar 2003). Owing to intra-arc extension and later obduction on the Indian lithosphere some time between 65 and 45 Ma, all crustal levels of the arc ranging from the upper mantle cumulates to the uppermost volcanic and sedimentary sequences are now exposed (Coward et al. 1986; Treloar et al. 1996; Searle et al. 1999; Burg et al. 2006).

The southern part of the Kohistan is comprised of the Jijal Complex and the Southern Amphibolites (collectively called the Southern Plutonic Complex) representing the base and lower/middle crust of the island arc, respectively (Figs. 1, 2) (Jan and Howie 1981; Jan and Windley 1990; Ringuette et al. 1999). It is separated from the northern part of the arc, the here called Gilgit Complex, by the Chilas Complex, a large ultramafic–mafic body assumed to have intruded during intra-arc rifting (Khan et al. 1989; Jagoutz et al. 2006; Jagoutz et al. 2007). The southern and central parts of the Gilgit Complex are occupied by the Kohistan batholith, dominantly composed of plutonic rocks with screens of volcanic and sedimentary rocks and their metamorphosed equivalents (Petterson and Windley 1985; Pudsey et al. 1985). The Northern part of the Gilgit Complex is made up by various volcanic sequences (Chalt, Shamran, Teru) and sediments (Yasin).

The Chilas Complex has a composition akin to bulk lower continental crust (Jagoutz et al. 2006) and is therefore inadequate as a complement of the upper crust granitoids exposed in the Kohistan batholith. Despite the large size of the Chilas Complex (Fig. 1), available U–Pb zircon ages document a rather limited time span of emplacement around 85 Ma (Zeitler 1985; Schaltegger

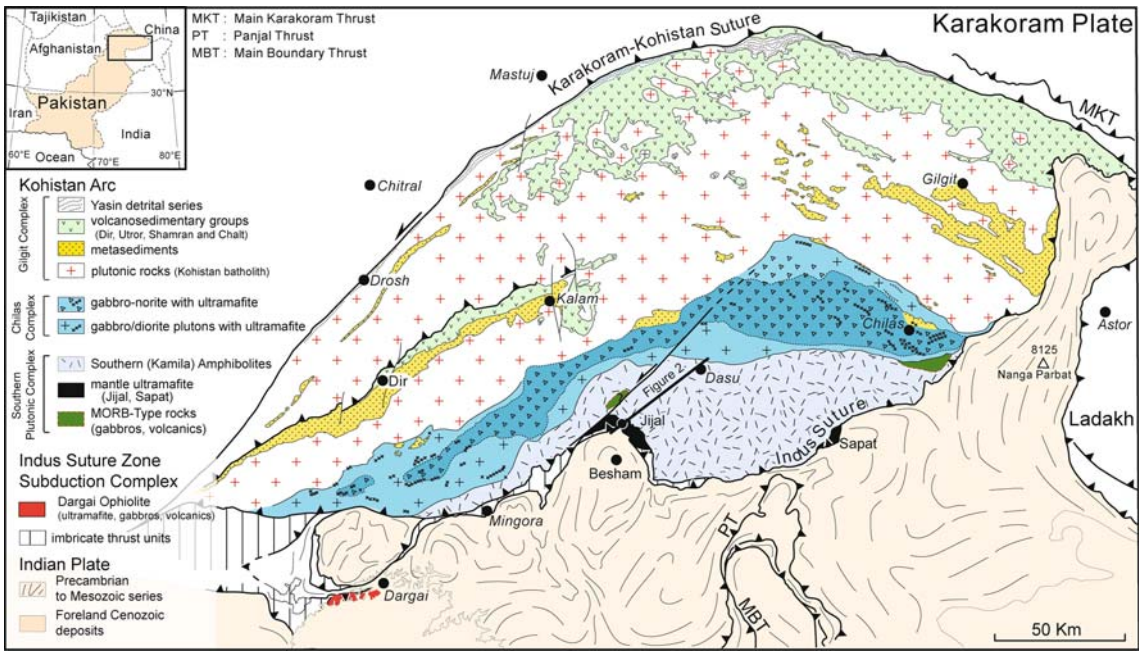

Fig. 1 Geological map of the Kohistan arc (work in progress). The map is based on own field observation and remote sensing of Landsat ETM + 7 pictures (band combination 743 and a principal component picture of the same bands). The location of Fig. 2 is indicated

et al. 2002). By contrast, the magmatic activity is significantly longer in the Southern Plutonic Complex [≥120–70 Ma (Yamamoto and Nakamura 1996; Yamamoto and Nakamura 2000; Schaltegger et al. 2002; Yamamoto et al. 2005)] and the Kohistan batholith (154–30 Ma, Petterson and Windley 1985; Schaltegger et al. 2004; Jagoutz et al. 2009). As the ultramafic cumulates and the lower mafic parts of the Southern Plutonic Complex are depleted in incompatible elements (Garrido et al. 2006; Dhuime et al. 2007, 2009), they potentially are adequate complement to upper crustal granitoids.

In the first paper (Jagoutz et al. 2009), we have presented geochronological data showing that the granitoids in Kohistan were formed during a steady-state process and are temporally unrelated to intrusion of the voluminous Chilas Complex mafic magmas. This implies that the formation mechanism of these granitoids was a constant process and is not related to a singular event as would be expected if granitoid formation is triggered by the emplacement of large masses of mafic melts like the Chilas Complex. Based on geochemical data, we concluded that the major and trace element characteristics of the arc granitoids involve the fractionation of amphibole. Amphibole is a major constituent mineral in the ultramafic rocks and the lower crustal gabbros of the Southern Plutonic Complex.

Field observations and rock analyses from the lower part of the Southern Plutonic Complex were used to constrain the fractionation sequence, volume, and composition for the fractionation model presented in this publication. Accordingly, I first present a brief field description of the key lithologies in the Southern Plutonic Complex from the deepest to the shallowest part, i.e., from south to north (Fig. 2). More details can be found in Burg et al. (2005) and detailed petrological description can be found in (Jan and Howie 1981; Miller et al. 1991; Miller and Christensen 1994; Ringuette et al. 1999).

Ultramafic suite

The ultramafic cumulate suite is dominated by olivine- and clinopyroxene-rich lithologies (dunite, wherlite, olivine-clinopyroxenite and (ol)-websterite locally with tiny amounts of garnet) (Figs. 2, 3). Harzburgite, i.e., possible residual mantle, is described in the Jijal section but was not observed in the transect studied (Jan and Howie 1981; Miller et al. 1991). Dunite, widespread in the partly serpentinized lower part of the section, decreases in abundance up section. Various modal amounts of olivine and pyroxene define compositional banding. Dunite flames of various sizes (centimeter to meter) are relict within pyroxene-rich ultramafic rocks. Cr-diopside-rich dykes crosscut spinel bands within dunite bodies tens of meters across, whereas meter-sized dis- and concordant dunite bodies are present. Discordant ones cut the compositional banding of pyroxene-rich rocks. Amphibole becomes increasingly abundant up section and pyroxene-rich ultramafic rocks grade into hornblende-, clinopyroxene- and garnet-rich rocks. Modal variations are pronounced and rock-types vary from hornblendite to garnetite and pyroxenite within centimeter

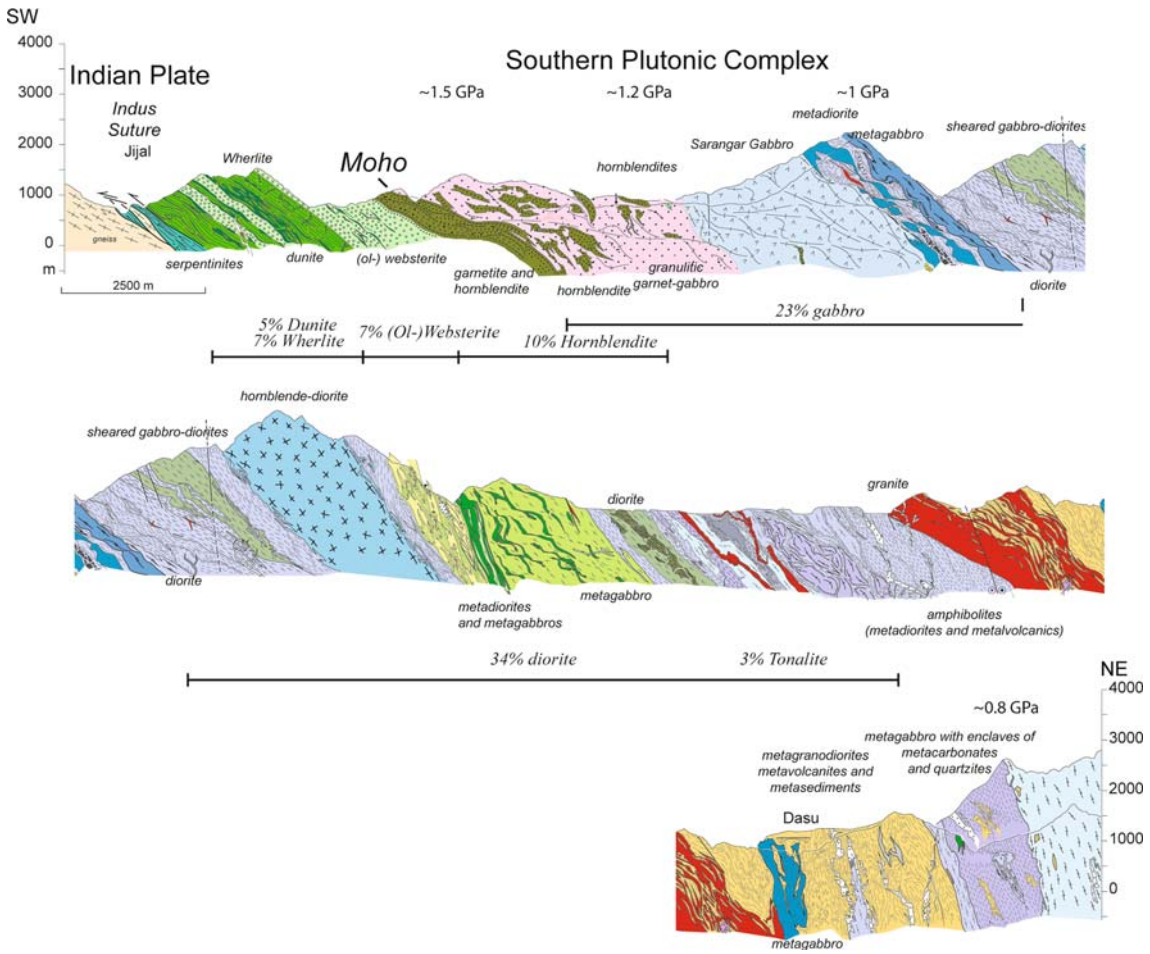

Fig. 2 Cross section through the Southern Plutonic Complex (simplified after Burg et al. 2005). Shown are the relative proportions of the main units that have been used to infer relative rock volumes used in the model. Petrological geobarometer estimates are shown at their approximate locations (Yamamoto 1993; Yamamoto and Yoshino 1998; Yoshino et al. 1998)

to outcrop scales (Fig. 3). These modal variations occur as confined bands/dykes or as diffuse schlieren, whereas the transition between both occurrences takes place over few centimeters. The replacive relationships between pyroxene-rich ultramafic and dunite and the irregular transition from schlieren to dyke-shaped garnetite and hornblendite are interpreted as indicating numerous percolative intrusive events and associated fractionation and melt-rock reactions within a semi-consolidated crystal mush.

The lower/middle crust

The first occurrence of massive volumes of plagioclase defines a sharp, intrusive contact of a garnet-bearing (meta-) gabbro into underlying ultramafic rocks; this contact is inferred to be the sub-arc Moho (Miller and Christensen 1994). Outcrop-scale modal variation of garnet within the granulite-facies garnet-gabbro is pronounced ranging from garnetite to rare garnet-free gabbro, but on average garnet constitutes ~20–30 vol% of the rock and the remaining mineralogy is dominantly composed of plagioclase, clinopyroxene, amphibole, oxides and ± epidote and paragonite (Fig. 3). The rocks generally have significant amount of quartz (up to 10%) even though the total whole rock silica content is low (~46–52 wt%, own unpublished data and Garrido et al. 2006; Dhuime et al. 2007). Up to hundred meters sized hornblendite bodies occur throughout the garnet gabbro. Contact relationships indicate the presence of older enclaves and younger dikes. Upsection, the garnet-bearing gabbro is overlain by the 98.9 ± 0.4 Ma (Schaltegger et al. 2002) Sarangar metagabbro which intrudes the garnet-bearing gabbros (Arbaret et al. 2000; Burg et al. 2005). The Sarangar gabbro forms the lowest part of the Southern Amphibolites (Burg et al. 2005) and corresponds to the Patan Complex of Miller et al. (1991). At the contact between Sarangar gabbro and garnet-gabbro, a complicated network of amphibole-rich zones and garnet-rich zones are present which has been attributed to fluid induced reaction (Yoshino et al. 1998) or partial melting (Garrido et al. 2006).

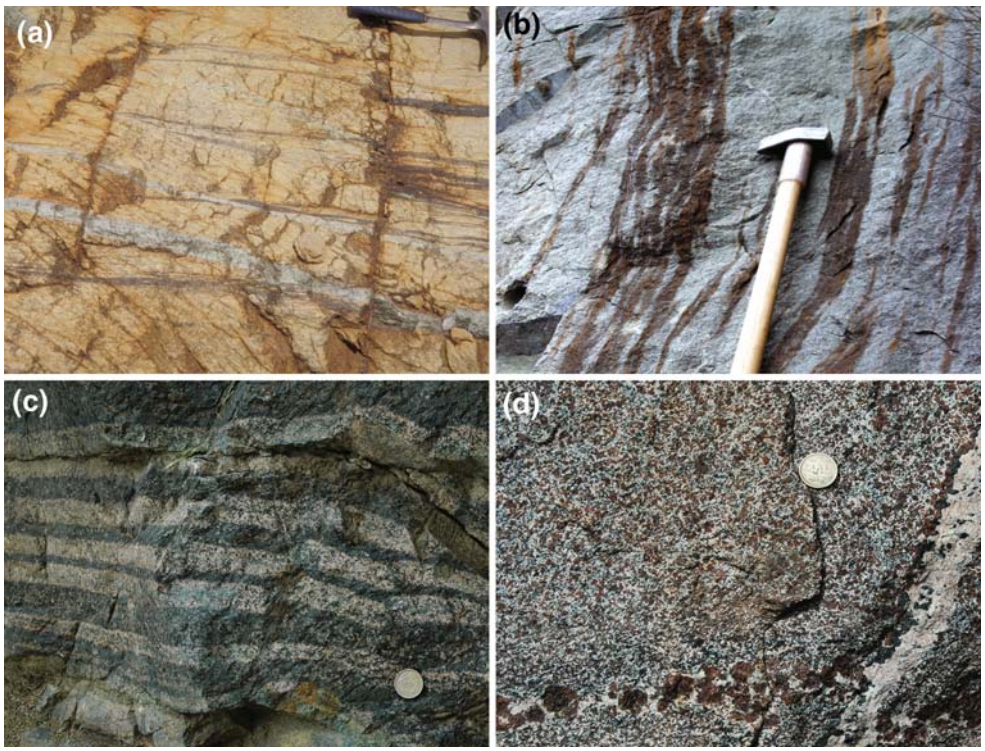

Fig. 3 Field relationships in the lowest part of the Kohistan arc. **a** Crosscutting relationship between Cr-diopside dykes and chromite layers in dunite. **b** Dunite "flames" are frequently observed in wherlite and websterite rocks in the ultramafic cumulates. Cross cutting and replacive structures are frequent in the ultramafic section indicating that the segment reflects a zone of melt percolation, fractionation, and reaction. **c** Magmatic banding defined by modal variability of garnet and hornblende in the hornblendite/garnetite-rich upper part of the ultramafic cumulates. **d** Garnet-rich gabbroic rock from the lower crust

The Sarangar gabbro itself is intruded by hornblendite and tonalitic dykes dissected by spectacular anastomosing shear zones around meter-scale lenses in which magmatic fabric is preserved (Arbaret et al. 2000). The Sarangar gabbro is separated by a magmatic breccia from the middle part of the Southern Amphibolites, the so-called Kiru amphibolites. The strongly sheared amphibolite-facies sequence comprises mutually intrusive, variously deformed meta-gabbros, diorites, tonalites and minor hornblendites, and plagioclase-quartz-amphibole pegmatites. Calc-silicate enclaves are locally present (Yoshino and Satish 2001).

The uppermost portion of the Southern Amphibolite, the Kamila amphibolites of Treloar et al. (1996), is a sequence of various plutonic bodies with gabbroic, dioritic, tonalitic, and granitic composition intruding into a lower amphibolite-facies volcano-sedimentary sequence. A granite has been dated at 97.1 ± 0.2 Ma (Schaltegger et al. 2002). To the north the Chilas Complex intrudes the Kamila sequence.

The pressure estimates for the lower part of the arc vary significantly, but the average of well-constrained geobarometer constraints from mineral rim composition constrains the formation depth of the MOHO to around ~1.5 GPa. The metavolcanics at the top of the section record pressures of ~0.8 GPa (Fig. 2) (Yamamoto 1993; Yoshino et al. 1998; Ringuette et al. 1999; Yoshino and Okudaira 2004). Even though the pressure difference between the base of the arc and the top of the Complex (~0.7 GPa) correlates well with the mapped thickness (~26 km), the relation between the mapped thickness of single units and geobarometric constraints vary significantly within the Complex (Fig. 2). Within the garnet gabbro (see below) the pressure decreases from 1.5 GPa at the base to 1.2 GPa at the top whereas the mapped thickness is only ~4.5 km. As the pressure "gap" is not associated with lithological boundaries or structural discontinuities, the observed mismatch likely is the result of homogenous thinning of the studied exposures, rather than due to missing section. This interpretation is supported by the detailed map of the area (Zeilinger 2002), which documents significant variability of the thickness of gabbroic units along strike.

Despite the well-exposed nature of the lower crust, the interpretation of the rock-forming mechanism in the Southern Plutonic Complex is debated. The sequence is either interpreted as the result of high-pressure crystallization of hydrous arc magmas (Miller et al. 1991; Ringuette et al. 1999; Müntener et al. 2001; Alonso-Perez et al. 2009) or as the result of metamorphic dehydration

reactions (Yamamoto and Yoshino 1998; Garrido et al. 2006). The discussion mainly circles around the interpretation of the origin of garnet in garnetite and in the gabbros, i.e., whether garnet is a metamorphic or magmatic phase.

Garnet is a major constituent of the Jijal section of Kohistan not only in the garnetite. The garnet modal abundance often exceeds 30% in gabbros, much less in silica-rich granitoids. Importantly, whereas garnetite and few primitive garnet gabbros have enriched whole rock HREE in accordance with textural evidence for magmatic garnet (Ringuette et al. 1999) some garnet-bearing gabbroic rocks from the Jijal section have metamorphic textures and unfractionated whole rock HREE patterns very similar to hornblende gabbros, which has been interpreted as evidence for some garnet in those rocks being a metamorphic phase (Yamamoto and Yoshino 1998; Garrido et al. 2006). This interpretation is in line with the fact that hornblende-rich gabbros with very similar major and trace element composition to the "garnet-gabbro" are found in the shallower levels of the Kohistan arc, e.g., in the vicinity of the Chilas complex (Jagoutz et al. 2006).

In this paper I follow the discussion outlined in Jagoutz et al. (2009) and interpret the rock series found in the Southern Plutonic Complex as dominantly formed by common crystal fractionation mechanisms (e.g., equilibrium, fractional, in situ fractionation and melt-rock reaction at decreasing melt mass).

Model setup

In the model presented, trace and major element variations are modeled by stepwise subtraction of cumulates of fixed composition (dunite, wherlite, oliv-websterite, hornblendite, gabbro, diorite, tonalite), rather than by the conventional use of mineral-melt partition and exchange coefficients and equations for fractional or equilibrium crystallization. This type of fractionation model has few distinctive advantages compared to more commonly used approaches as it allows to construct a model that is entirely constrained by field observation and composition from the Kohistan arc (see later). It is independent of the set of exchange or partition coefficients used, and assuming equilibrium, of the formation mechanism of the fractionated rocks (e.g., fractional or equilibrium crystallization, melt-rock reactions). Indeed, deep-seated cumulate rocks are generally not simple orthocumulates but are often more complex rocks with various amounts of trapped melt produced by circulating intercumulus liquids during more complex fractionation mechanism such as in situ fractionation (Jagoutz et al. 2006, 2007).

I assume mass balance whereby the parental melt, the cumulate, and the derivative melts are related by

$$\mathrm{Cm}_n = (\mathrm{Cm}_{n-1} - (X * C_\mathrm{c}))/(1 - X), \quad (1)$$

where Cm_n is the concentration of the element of interest in the fractionated melt at step n, Cm_{n-1} is the composition of the melt derived at step $n-1$, and C_c is the concentration of the element in the fractionating cumulate composition. Fractionation steps are 1%. $X = (X_{m-1} - X_m)/X_{m-1}$, where X_m is the percentage of melt remaining at the corresponding step, accounts for the decreasing melt mass during fractionation. C_c was constrained using the range of whole rock compositions of ultramafic, gabbro, and diorite from the Southern Plutonic Complex (own unpublished data and Garrido et al. 2006; Dhuime et al. 2007, 2009). Gabbroic, and to a lesser extent, dioritic rocks can range in character from primitive cumulates to "melt-like", which is often inferred from the trace element systematic. I used the presence of a positive Eu anomaly as a criterion to select rocks with a cumulative character and constrained the fractionated composition from those. Primitive arc magmas are scarce in the Kohistan arc, and volcanic rocks are often strongly altered reflected by low totals in the analyses. Therefore, as an initial parental melt composition (Cm_0) an averaged composition has been calculated from published, primitive high Mg# (>0.66) Kohistan arc magmas, rather than choosing a single whole rock composition. The resulting composition is basaltic (Table 1) with a high Mg# (0.7) and high Ni (168 ppm), appropriate for melts in equilibrium with an olivine-dominated mantle assemblage. The trace element composition has been similarly average from published data and the data set has been filtered for outliers. Published trace element data in Kohistan is, however, of variable quality and very few primitive samples have high-quality trace element data making the averaged composition rely on a very small dataset. For trace elements for which the averaged concentration was unrealistic (e.g., $\mathrm{Sr}_{\mathrm{Kohistan}}$ average = 133 ppm compared to 306 ppm for the average oceanic primitive melt Kelemen et al. 2003a), values for primitive oceanic arc magmas as compiled by Kelemen et al. (2003a) (see Table 1) were used.

Seven fractionation steps were calculated whereby the cumulate composition was successively changed from dunite, wherlite (ol-) websterite, hornblendite (garnet/hornblende-) gabbro to diorite and tonalite. For the model presented here, the composition of the garnet-"gabbro" was used to keep the model associated with the field constraints. However, the major geochemical characteristics of arc granitoids could equally be modeled by fractionation of primitive hornblende-gabbro. Naturally, fractionation of magmatic garnet will strongly influence the HREE characteristic. The role of magmatic garnet will be discussed in detail later.

Table 1 Compositions used for the model compared with the averaged analyzed whole rock composition and results of the fractionation model

	Parental melt[a]		Fractionated cummulate phases														
		N	Dunite[b]	Dunite[c] $N = 6$	2σ	Wherlite[b]	Wherlite[c] $N = 4$	2σ	Websterite[b]	Websterite[c] $N = 7$	2σ	Hornblendite[b]	Hornblendite[c] $N = 4$	2σ	Gabbro[b]	Gabbro[c] $N = 16$	2σ
SiO_2	50.72	14	39.55	41.10	2.99	48.46	49.37	3.21	51.60	51.87	1.77	42.16	42.80	1.88	45.76	46.24	6.94
TiO_2	0.80	14	0.03	0.03	0.06	0.06	0.04	0.05	0.30	0.17	0.17	1.79	1.46	1.06	0.78	0.79	0.53
Cr_2O_3	0.06	14	0.64	0.67	0.51	0.46	0.12	0.48	0.04	0.31	0.49	–	0.02	0.03	–	–	–
Al_2O_3	15.67	14	0.56	0.58	0.98	0.47	1.21	2.06	6.09	3.42	2.80	16.97	15.90	3.12	20.24	20.00	2.10
FeOT	8.60	14	10.12	11.27	4.62	6.88	7.59	2.67	5.90	6.55	2.41	11.88	12.36	2.98	11.75	11.87	4.04
MnO	0.17	14	0.14	0.15	0.06	0.13	0.14	0.20	0.13	0.13	0.06	0.10	0.11	0.05	0.24	0.25	0.18
MgO	10.87	14	48.21	45.44	5.92	32.44	31.68	5.36	18.78	19.57	6.60	13.05	12.93	1.20	7.19	6.88	2.86
CaO	9.88	14	0.64	0.67	0.69	10.62	9.65	3.79	17.06	17.85	7.02	11.39	11.91	0.88	12.08	12.20	2.71
Na_2O	2.43	14	0.10	0.10	0.06	0.49	0.16	0.45	0.08	0.12	0.10	2.25	2.25	0.51	1.67	1.69	1.10
K_2O	0.61	14	–	–	–	–	–	–	–	–	–	0.39	0.22	0.14	0.08	0.08	0.08
P_2O_5	0.19	14	–	–	–	–	–	–	–	–	–	0.02	0.02	0.01	0.20	–	–
Total	100		100	100		100	100		100	100		100	100		100	100	
Mg#	0.69		0.89	0.89	0.70	0.89	0.88		0.85	0.84		0.66	0.65		0.52	0.51	
Rb	*9.89*	–	0.039	0.039	0.040	0.069	0.069	0.102	0.101	0.101	0.181	0.719	0.719	0.407	0.531	0.531	0.651
Sr	*306*	–	0.591	0.591	0.656	6.04	6.04	1.74	8.86	8.86	6.92	166	166	69	230	230	161
Y	11.3	8	0.043	0.043	0.028	0.494	0.494	0.441	2.54	2.535	3.82	8.40	7.30	6.33	14.29	14.29	12.02
Zr	*40.0*	–	0.026	0.026	0.031	0.116	0.116	0.037	0.514	0.514	1.154	5.13	8.455	16.43	5.43	5.43	3.51
Nb	1.94	9	0.028	0.028	0.022	0.030	0.030	0.014	0.024	0.024	0.016	0.299	0.299	0.220	0.209	0.21	0.25
Ba	*131*	–	0.602	0.602	1.677	1.564	1.564	2.595	3.09	3.086	6.67	27.7	27.75	15.9	31.8	31.8	30.3
La	*5.98*	–	0.001	0.001	0.001	0.029	0.029	0.003	0.070	0.052	0.063	0.463	0.463	0.366	1.22	1.22	1.90
Ce	*14.4*	–	0.008	0.008	0.005	0.069	0.069	0.028	0.156	0.156	0.204	2.05	2.051	1.47	3.11	3.11	4.22
Nd	*8.8*	–	0.008	0.008	0.005	0.085	0.085	0.079	0.328	0.328	0.440	3.59	3.586	2.37	3.07	3.07	2.70
Sm	*2.33*	–	0.008	0.008	0.003	0.042	0.042	0.040	0.195	0.195	0.266	1.67	1.439	0.89	1.18	1.18	0.696
Eu	*0.800*	–	0.003	0.003	0.001	0.020	0.020	0.017	0.095	0.095	0.129	0.643	0.643	0.302	0.692	0.69	0.287
Gd	*2.28*	–	0.009	0.009	0.003	0.074	0.074	0.083	0.373	0.373	0.515	1.87	1.865	1.18	1.98	1.98	0.710
Dy	*2.81*	–	0.011	0.011	0.006	0.108	0.108	0.106	0.547	0.547	0.744	1.75	1.755	1.22	2.65	2.65	1.56
Er	*1.36*	–	0.009	0.009	0.002	0.068	0.068	0.052	0.333	0.333	0.425	0.814	0.814	0.620	1.78	1.78	1.21
Yb	*1.83*	–	0.012	0.012	0.004	0.068	0.068	0.039	0.287	0.287	0.355	0.605	0.605	0.497	1.35	1.35	1.07
Lu	0.264	8	0.003	0.003	0.000	0.012	0.012	0.006	0.046	0.046	0.055	0.088	0.088	0.072	0.299	0.299	0.206
Hf	1.08	8	0.004	0.004	0.002	0.008	0.008	0.003	0.035	0.035	0.069	0.373	0.373	0.319	0.211	0.224	0.176
Ta	0.151	8	0.001	0.001	0.001	0.002	0.002	0.002	0.001	0.010	0.026	0.019	0.019	0.014	0.016	0.016	0.014
Pb	*2.480*	–	0.071	0.071	0.086	0.245	0.245	0.300	0.125	0.125	0.115	0.240	0.240	0.094	0.471	0.515	0.617
Th	0.89	8	0.002	0.002	0.001	0.005	0.005	0.006	0.003	0.003	0.003	0.004	0.004	0.003	0.009	0.009	0.007
U	0.289	7	0.002	0.002	0.001	0.005	0.005	0.008	0.004	0.004	0.004	0.002	0.002	0.002	0.014	0.014	0.026

Table 1 continued

						Calculated liquid compositions						
	Diorite[b]	Diorite[c]	2σ	Tonalite	Assimilated liquid[d]	Fractionation model (in percent crystallized)				Fractionation + assimilation		
		$N = 13$				10%	30%	60%	80%	30% frac + 5% assim	60%	80%
SiO_2	52.74	54.39	1.86	71.06	71.72	51.44	52.94	57.07	61.40	54.11	59.93	66.58
TiO_2	1.00	0.92	0.25	0.46	0.03	0.88	0.83	0.82	0.64	0.79	0.74	0.49
Cr_2O_3	–	–	–	–	–	0.01	–	–	–	–	–	–
Al_2O_3	19.55	17.98	2.06	16.75	15.87	17.27	19.04	18.26	16.97	18.94	17.95	16.28
FeOT	7.87	9.06	0.95	1.93	1.36	8.61	8.44	6.66	5.45	8.10	5.74	3.63
MnO	0.05	0.18	0.06	0.07	0.07	0.18	0.19	0.19	0.33	0.01	0.01	0.01
MgO	4.73	4.79	1.34	0.49	0.46	7.74	4.93	3.68	2.63	4.71	3.07	1.44
CaO	10.07	9.70	2.53	3.66	3.39	10.34	9.52	7.96	5.86	9.24	7.17	4.31
Na_2O	3.31	2.46	1.67	3.86	1.94	2.66	3.05	3.79	4.27	3.01	3.82	4.30
K_2O	0.53	0.34	0.23	1.42	5.16	0.67	0.80	1.27	2.00	1.03	1.77	2.97
P_2O_5	0.14	0.17	0.12	0.30	0.00	0.21	0.26	0.32	0.50	0.07	0.00	0.00
Total	100	100		100	100	100	100	100	100	100	100	100
Mg#	0.52	0.49		0.31	0.37	0.62	0.51	0.50	0.46	0.51	0.49	0.41
Rb	1.59	1.59	1.97	11.1	108	10.9	13.9	23.9	46.1	18.8	34.7	67.2
Sr	323	323	263	431	380	338	408	526	729	407	543	758
Y	17.8	19.2	12.8	1.92	10.0	12.5	14.5	14.0	10.2	14.3	13.5	9.2
Zr	48.2	48.2	37.5	263	48.2	44.2	56.0	86.3	124	55.6	90.4	132
Nb	1.759	1.759	1.860	2.09	-	2.14	2.70	4.30	6.8	2.88	4.89	8.0
Ba	94.3	94.3	90.0	232	624	145	182	283	472	204	343	587
La	6.67	6.67	3.23	8.53	12.3	6.61	8.42	12.8	19.0	8.62	14.0	21.1
Ce	15.81	15.81	8.06	14.3	21.0	15.9	20.1	30.6	45.4	20.2	32.4	48.7
Nd	10.53	10.53	5.83	4.70	8.26	9.73	11.93	17.23	23.94	11.74	17.73	24.80
Sm	3.75	2.82	1.64	0.703	1.48	2.57	3.04	3.96	4.17	2.95	3.95	4.15
Eu	1.288	1.048	0.468	0.545	1.49	0.88	1.03	1.17	1.06	1.05	1.24	1.19
Gd	3.65	3.46	1.78	0.444	1.51	2.52	2.92	3.31	2.97	2.84	3.23	2.82
Dy	3.86	3.86	1.74	0.332	1.63	3.10	3.66	4.20	4.55	3.56	4.09	4.32
Er	2.31	2.31	1.17	0.203	0.72	1.50	1.77	1.66	1.01	1.72	1.54	0.78
Yb	2.22	2.22	1.23	0.272	0.628	2.02	2.47	3.16	4.10	2.38	3.09	3.95
Lu	0.360	0.360	0.212	0.043	0.090	0.292	0.357	0.389	0.418	0.343	0.368	0.376
Hf	1.290			6.58	1.97	1.19	1.47	2.23	3.17	1.50	2.40	3.49
Ta	0.105	0.105	0.109	0.129	-	0.167	0.212	0.343	0.581	0.201	0.344	0.579
Pb	2.47	2.47	1.84	0.000	20.85	2.73	3.45	5.32	8.18	4.35	7.33	12.10
Th	0.215	0.215	0.353	0.406	0.49	0.99	1.27	2.18	4.15	1.23	2.26	4.26
U	0.073	0.073	0.098	0.079	0.265	0.319	0.409	0.70	1.32	0.402	0.73	1.38

[a] Number in italics corresponds to values from the average oceanic arc composition from Kelemen et al. (2003a)

[b] Composition used in the model calculation

[c] Average wholerock compostion of the rock-type (N = Number of whole rock analyses averaged)

[d] Rock composition of a leucocratic melt in migmatiszed metagreywake (sample C 227 from Jagoutz et al. 2009)

A general problem of such mass balance models is to estimate the amount of fractionated cumulate. The cumulate volumes were constrained dominantly from field observations [using own field observations and the relative proportion of the different units as documented in a detailed cross section of the Southern Plutonic Complex (Fig. 2)]. However, as the residual mantle is not preserved (?) in the section studied, we cannot assume that the ultramafic cumulate part is preserved in appropriate volumes compared to the overlying crust. Therefore, the volumes of ultramafics fractionated (i.e., before the onset of plagioclase fractionation) have been assumed to be 30%; this is towards the lower end of volumes inferred from geochemical constraints (Kay and Kay 1985). Additionally, the relative volumes of different ultramafic rocks were varied iteratively within the field constraints until an optimal fit between model and granitoid data was archived. These variations are, however, generally minor (>2–3%), and had only limited influence on the results and therefore only minor influence on the constraints. The relative volumes of gabbroic and dioritic rocks were determined as well based on field observation and correcting for the preserved pressure gap. I verified the cumulate volumes using olivine or clinopyroxene Mg# and calculating the $Mg\#_{melt}$ to approximate the fractionation steps (e.g., Greene et al. 2006). This proved to be difficult for Kohistan rocks as their clinopyroxene Mg# is affected by metamorphic reequilibration to higher Mg# (Jagoutz et al. 2007), especially for the ultramafic cumulate section. However, the lowest Mg# of clinopyroxene reported for the different lithologies (Jan and Howie 1981) generally matches well with a calculated $Mg\#_{melt}$ and the modeled composition with the exception of the most primitive rock. The match, however, becomes very good for the lower crustal gabbros. Finally, the dominant model results presented here used the following cumulate volumes: 5% dunite, 7% wherlite, 8% (ol-) websterite, 10% hornblendite/garnetite, 23% gabbro, and 34% diorite (Fig. 2). Correcting for the preserved pressure gap results in significantly higher proportions of gabbro fractionation ($\sim$46%) and lesser diorite ($\sim$8%). Regarding geochemical data (e.g., positive Eu/Eu* ($Eu/Eu^* = 2^*Eu_N/(Sm_N + Gd_N)$) indicating that some tonalite rocks are cumulates, I fractionated tonalite as the SiO_2 of the derivative liquid reaches 72 wt% as a minor final step (only in the model including the pressure corrected volumes or assimilation, see later). Calculations were carried out until 10% liquid mass remained.

Assimilation

Assimilation occurs throughout the crustal column, but for the model it was assumed to be a relevant crust-forming process within the lower crust only (Hildreth and Moorbath 1988). The reasoning is that (1) assimilation is most efficient under elevated ambient temperature and high magma temperature as common in the lower crust and (2) depleted residues potentially delaminate and sink into the mantle. In shallower crustal levels, assimilation is a crustal-reworking rather than crust-forming process as delamination of the restite is unlikely.

Pursuing this line of thought, I investigated the role of assimilation at Moho level, which coincides in Kohistan with the appearance of plagioclase (Miller and Christensen 1994). In the model, this level corresponds to melt compositions that have fractionated 30% of ultramafic, plagioclase-free cumulates (dunite, wherlite (ol)-websterite and hornblendite/garnetite). For the composition of the assimilated melt the composition of leucocratic melt patches in migmatitic rocks found in the vicinity of the Chilas Complex was used (Jagoutz et al. 2009).

The melt composition due to assimilation was calculated by

$$Cm_{mixed} = (X^*Cm_{30\%} + (1 - X^*C_{as})), \quad (2)$$

whereby $Cm_{30\%}$ is the concentration of the element of interest-after 30% fractionation, C_{as} is the concentration of the element in the assimilated melt, and X is the percentage of assimilated melt. Additionally, the increase in melt mass due to assimilation was accommodated. Subsequent fractionation steps (gabbro, diorite) were equal to those in the pure fractional crystallization model whereas the fractionation interval of tonalite is increased due to the increase in melt mass.

Mass balance constraints

To successfully model upper crustal granitoids not only the composition but also the observed volumes must be adequately reproduced. The upper crust is $\sim$30% of the bulk crust (Rudnick and Gao 2003). If these 30% of the crust are formed by mantle-derived melts, the observed volumes pose a mass balance constraint. As in the model, mantle-derived melts fractionate 30% below the seismic MOHO and the remaining 70% make up the continental crust. Accordingly, the remaining melt should reach mean upper crustal composition after $\sim$ 80% fractionation to satisfy this mass balance constraint.

Results

The major and trace element composition of the parental melt, the fractionated cumulates (normalized to 100%) and the resulting composition of the derivative melt after 10, 30, 60, 80% fractionation and assimilation are given in

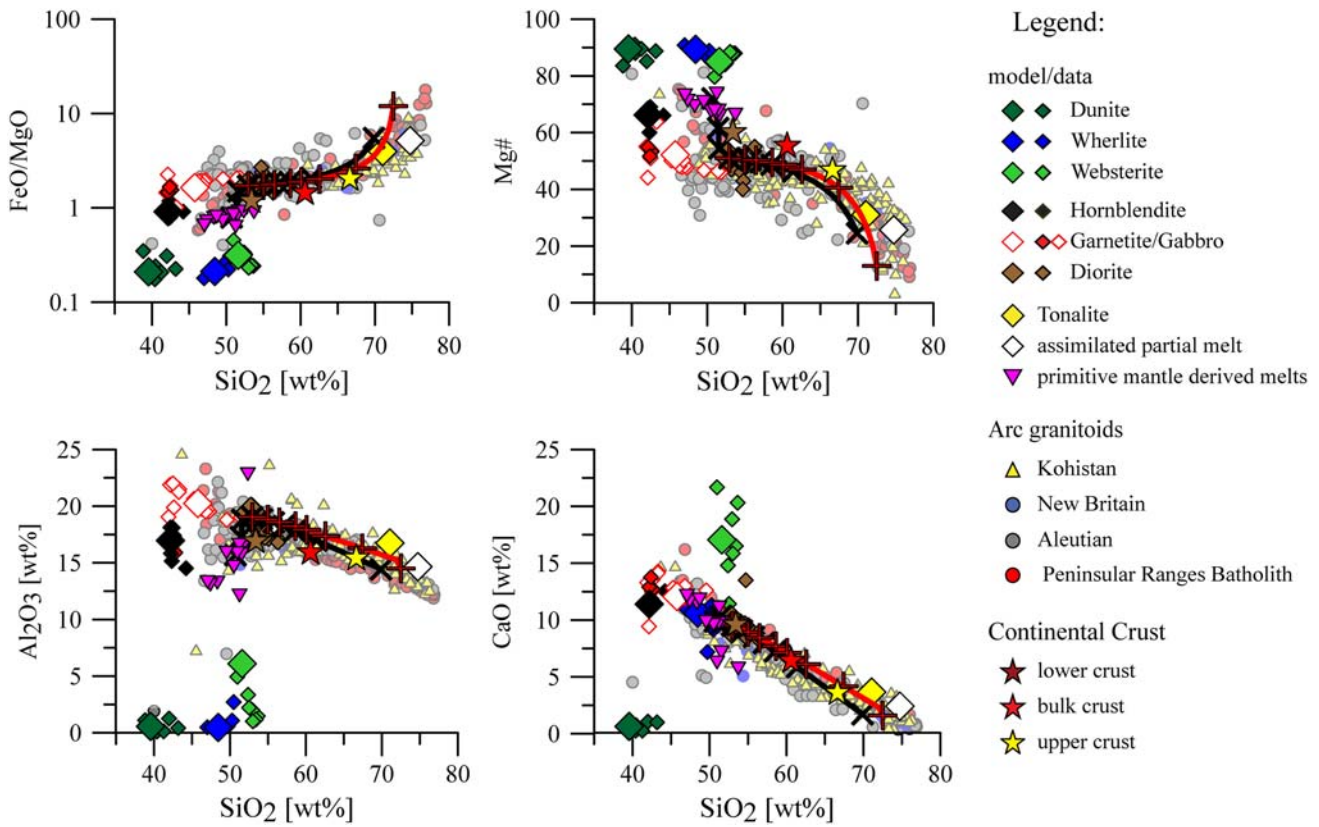

Fig. 4 Results of the fractionation and assimilation model described in the text. Two model results are shown. The *black line* illustrates the liquid line of descent calculated by the fractional crystallization model and the *red line* is a fractional crystallization model with 5% of the melt mass assimilated at the MOHO depth (i.e., at the onset of plagioclase fractionation) after initial 30% fractional crystallization below the MOHO. Crosses indicate 10% fractionation steps. The *larger diamond symbols* indicate the fractionated cumulate composition and the *smaller symbols* of the appropriate color illustrate the measured Kohistan whole rock compositions. The assimilated melt composition is a leucosome from a migmatitic meta-graywacke (Jagoutz et al. 2009). The evolution trend of the model is compared to trends in granitoids from oceanic arcs (Kohistan data as compiled by Jagoutz et al. 2009 and from Enggist (2007); Aleutian (excluding the continental part) and New England data are compilations from GEOREF) and continental arc [Western Peninsular Range batholith (Lee et al. 2007)], ultramafic and mafic rocks (*small diamonds*) are from the lower crust of the Kohistan arc (own unpublished data and Garrido et al. 2006; Dhuime et al. 2007, 2009). Primitive Kohistan arc magmas are volcanic whole rock compositions with high Mg# (>66) compiled from the literature (Shah and Shervais 1999; Bignold and Treloar 2003; Khan et al. 2008). *Brown, red, and yellow stars* indicate the composition of lower, bulk, and upper continental crust, respectively (from Rudnick and Gao 2003). *Symbols* in subsequent figures are the same

Table 1. The fractionated cumulate composition is shown in comparison with averaged measured whole rock compositions. Additionally, the trends for a fractional crystallization using the field-constrained volumes and a trend with 5% assimilation are compared to the whole rock composition from Kohistan and granitoids from oceanic arcs (Aleutian, New Britain) and from the Peninsular range batholith in Figs. 5, 6, 7, 8, 9, 10, and 11. As the fractionation trend using the volumes derived from pressure correction for gabbro (43%) and diorite (8%) is comparable to the trend, which includes assimilation, the former trend is omitted in the presented plots to preserve clarity. In general granitoids from different arcs do not differ dramatically in major and trace element chemistry (with the exception of a possible difference in K/Rb between island arc and continental arc granitoids, Kay et al. 1990), so that the inference drawn here is extended to upper continental crust formation in subduction zone settings in general.

Beginning from a primitive basaltic average Kohistan parental magma composition, the model successfully reproduces the main major and trace element characteristics of subduction zone granitoids and the major element composition of the bulk upper continental crust (Figs. 4, 5).

Even though fractionation is capable to explain the general trends observed in arcs, granitoid assimilation or the high volumes inferred by pressure corrections are essential to fulfill the mass balance stated above. Using the non-pressure corrected volumes and silica enrichment as an example, the calculated derivative melt after 80% fractionation has a silica concentration of 61 wt% less than the average upper crustal SiO_2 concentration (66.62 wt%, Rudnick and Gao 2003). Involving a limited amount of assimilation (5%) and/or the

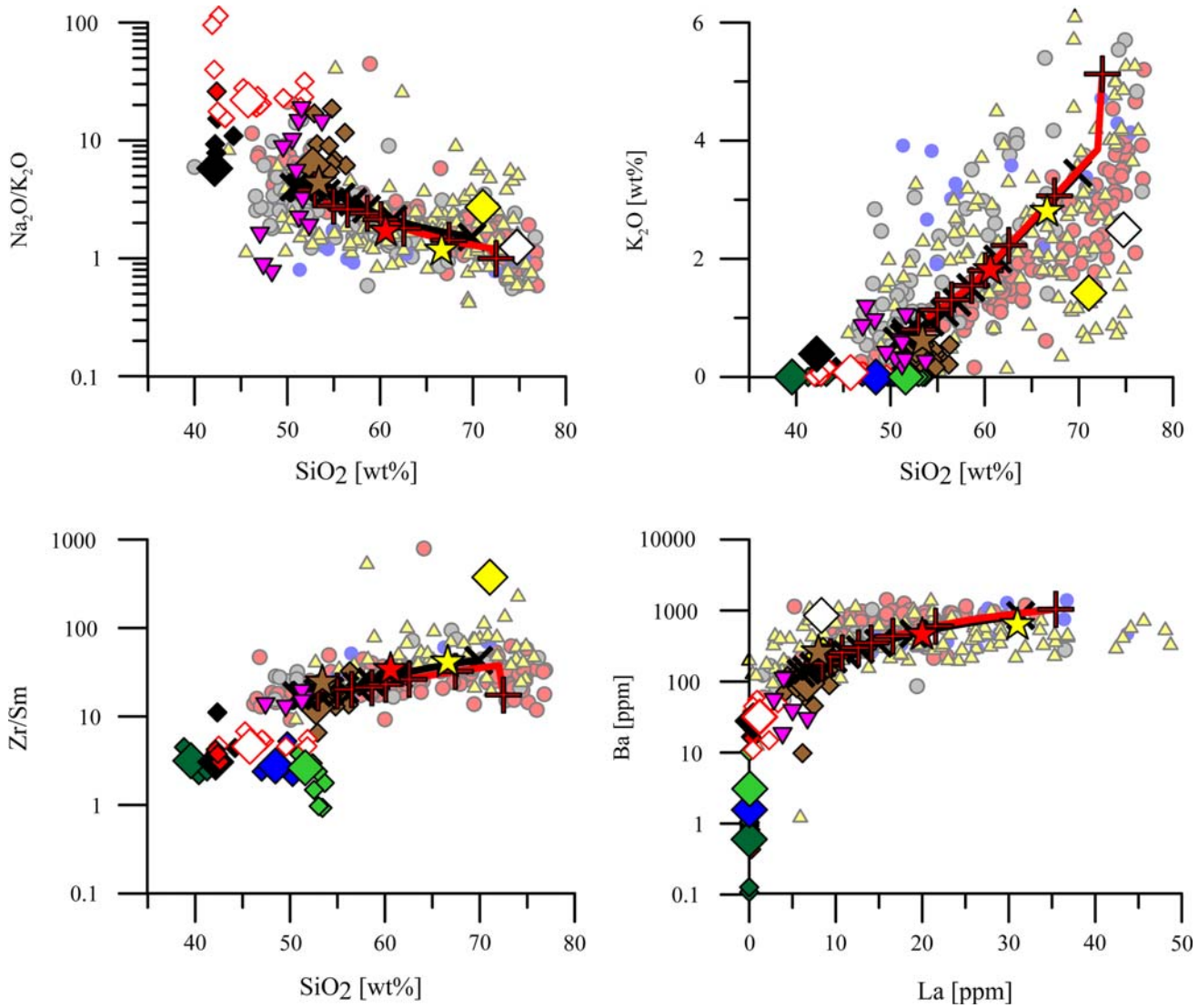

Fig. 5 Additional results from the model calculation for major and trace elements

pressure corrected cumulate compositions, are highly effective. In that case the derivative melt after 80% fractionation has a SiO_2 concentration of ~67 wt%. Accordingly, the presented model fulfills the mass balance constrained outlined above only by including large volumes of silica-poor gabbroic rocks or assimilation albeit only very limited amounts of the later is necessary. This documents that assimilation might be volumetrically significantly less pronounced than generally assumed, but it remains an important crust-forming mechanism under specific conditions to explain the volumes of the upper crust.

In the differentiation model the gabbro and diorite separation accounts for most of the silica-enrichment. Accordingly, I varied the composition of the gabbroic/dioritic composition to investigate the effect. Using more silica-rich compositions, the overall fractionation trend remains similar, but fractionation is significantly less effective in producing SiO_2-rich compositions. As a result, it is difficult to reproduce the volumes of upper crustal rocks even when using the pressure-corrected fractionated volumes. As an example, using a diorite composition with a SiO_2 content of 55 wt% the SiO_2 concentration of the derivative liquid after 80% fractionation is only 58.8 wt%, respectively 62 wt% using the pressure-corrected volumes; in both cases, significantly lower than the average upper crustal composition. However, only limited increase of assimilation, in this example, ~8–9% in both cases, is sufficient to derive upper crustal composition after 80% fractionation. Such limited amount of assimilation is well within the line of assimilation indicated by $\delta^{18}O$ (<~20%) for granitoids (e.g., Kemp et al. 2007). Isotopic trace elements (Sr, Nd, Pb) often indicate significantly higher crustal contribution to granitoids. Those data strictly only document the involvement of crustal, e.g., $^{87/86}Sr$ to the Sr

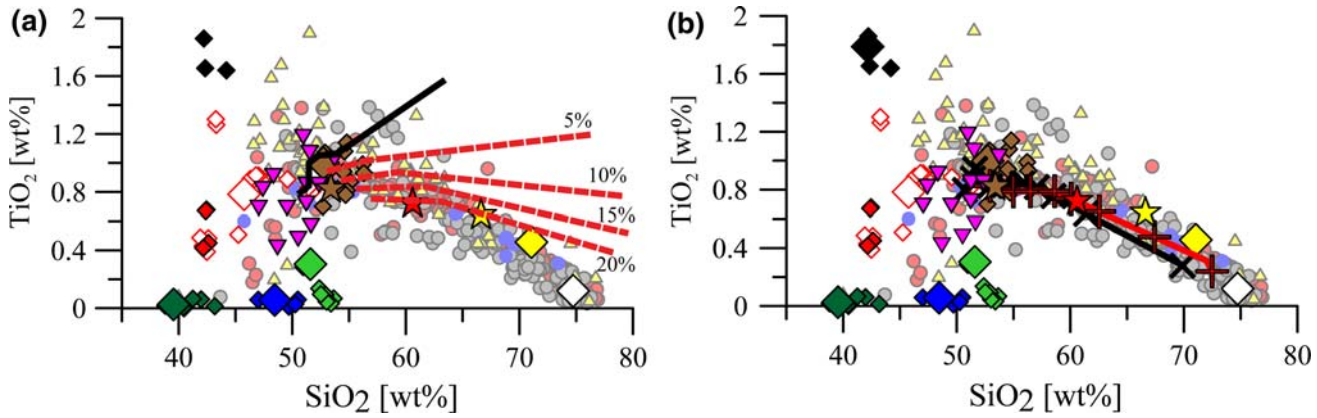

Fig. 6 SiO_2 versus TiO_2 document the importance of a low SiO_2/high TiO_2 composition to explain the overall compatible behavior of TiO_2 during granitoid evolution. **a** In a fractionation model calculated without hornblendite (low SiO_2/high TiO_2) fractionation TiO_2 remains overall incompatible. The compatible behavior of TiO_2 found in arc granitoids can only be poorly reproduced by assimilation of a high SiO_2/low TiO_2 composition (*white diamond*) shown here for 5, 10, 15, and 20% assimilation. **b** Alternatively, few percent fractionation of the hornblendite (10%) in accordance with field observations is capable to reproduce the compatible trend of the granitoids, with or without subsequent assimilation

budget and it is difficult to correlate the concentration of a trace element to volumes. In the example chosen here, assimilation of 9% changes the Pb concentration by 20% and affects only marginally the Sr budget (~1%). Different transfer agent, e.g., partial melts or bulk rock digestion, etc., will affect different isotopic trace element tracers to a variable degree, making the quantification of the volume of assimilation challenging. More reliable are major elements tracers such as oxygen.

Role of fractionating cumulates

A general problem for silica-enrichment by pure fractional crystallization mechanism is the "gabbro-barrier": Primitive cumulative gabbros (with positive Eu/Eu* anomaly, etc.) and pyroxenites have SiO_2 concentration in the range of 48–54 wt% comparable to basaltic to basaltic-andesitic melt compositions. Therefore, early appearance of plagioclase and pyroxene in the fractionation sequence is inefficient to produce volumetrically significant silica-rich derivative liquids as cumulates and melts can have very similar silica concentrations (e.g., Davidson et al. 2007). Even for parental melts with higher initial silica concentration (e.g., high Mg# andesites, Kelemen 1995) silica-enrichment due to gabbro fractionation is only marginally sufficient to produce silica-rich compositions and simultaneously fulfill the mass balance constraints of the upper crust. An important fractionation step for significant silica-enrichment and also for the behavior of certain crucial elements (e.g., TiO_2, see later) in the model is the fractionation of silica-poor minerals like amphibole, garnet, oxides, and An-rich plagioclase. Lithologies composed of these minerals (hornblendite, garnetite and garnet/hornblende gabbro) are found in the lower part of the arc. Whereas the origin of the garnet in the Southern Plutonic Complex is discussed (see above), the hornblende in hornblendite is generally assumed to be of magmatic origin. Therefore, I focused on hornblendite in the model. Hornblendites are found as a ~1 km thick layer below the Moho at the base of the Kohistan arc and as numerous, km-scale dykes and patches within the lower crustal garnet-gabbro (Burg et al. 2005). These rocks have Mg# intermediate between the olivine- and pyroxene-dominated ultramafic and the gabbroic rocks (Table 1). The SiO_2 whole rock concentration is very low, resembling the low-silica concentration of the constituent minerals. If such compositions are fractionated from a mantle-derived melt, they are highly effective in increasing the SiO_2 content of the residual liquids. In the model, fractionation of a few percent (~10%) is sufficient to push derivative liquids to sufficiently silica-enriched compositions such that subsequent gabbro fractionation produces volumetrically important silica-rich derivative liquids. Garnetites are equally effective. These results are in-line with hydrous moderate-to high-pressure fractional crystallization experiments that have shown that hornblende and garnet can be a magmatic phase in the lower crust at pressure and water content relevant to arcs (Müntener et al. 2001; Sisson et al. 2005; Alonso-Perez et al. 2009).

Certain oxides (e.g., CaO, Al_2O_3 and TiO_2) are crucial for determining the proportion and composition of cumulate phases and the parental magma composition. TiO_2 is an example: initially incompatible, in accordance with fractionation of olivine- and pyroxene-dominated cumulates that generally have low TiO_2 concentrations (<0.2 wt% on average), TiO_2 becomes compatible for the remaining fractionation sequence (Fig. 6). Thus, the TiO_2 content of the derivative liquids decreases. Yet, lower crustal gabbros in Kohistan generally contain the same

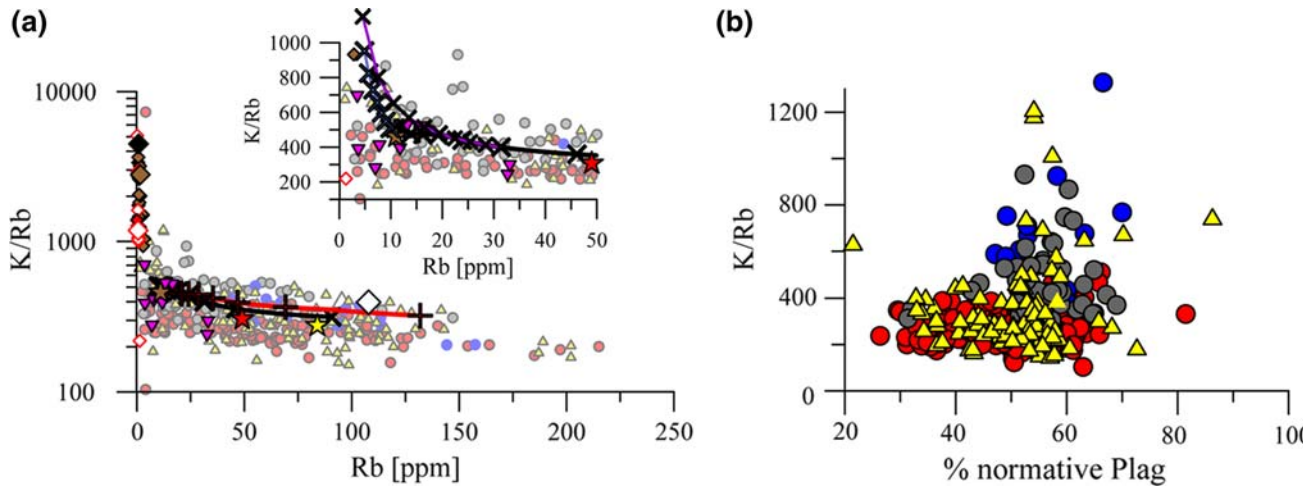

Fig. 7 Model results for K/Rb versus Rb. **a** The trend of the majority of the granitoids can be explained by fractionation. The decrease in K/Rb ratio at low Rb concentration, often inferred to be an assimilation signature, results from the early fractionation of hornblendite. However, highly elevated K/Rb ratios at low Rb concentration found in some arc granitoids (*small inset*) could be indicative of bulk rock assimilation. In that case the assimilated component must have a very different composition than the partial melt used in this model (*white diamond*). The *inset* shows trends of assimilation of a high K/Rb low Rb component (diorite) by a primitive and a highly fractionated (70%) melt. The assimilation trends in the inset only poorly reproduce the observed compositions and additionally indicate very high percentage of assimilation (crosses indicate 10% assimilation). Alternatively, high K/Rb ratios could be the result of accumulation processes of, e.g., plagioclase, biotite etc. Rocks with high K/Rb ratios have higher normative plagioclase content than rocks with low K/Rb (**b**)

amount of TiO_2 as the initial parental liquids ($\sim$0.8 wt%, see Table 1). Hence, the fractionation of such gabbroic compositions following the fractionation of the olivine- and pyroxene-dominated cumulates would result in an overall incompatible behavior of TiO_2 in derivative liquids (Fig. 6a). The compatible behavior of TiO_2 is also difficult to explain by assimilation of a high-SiO_2 low-TiO_2 melt composition (Fig. 6a). To produce the overall compatible behavior significant assimilation (>20%) is necessary, which is difficult to concur with melting models for the lower crust (Dufek and Bergantz 2005). Additionally, a poor match between model liquids and whole rock arc granitoids is observed. Alternatively, fractionation of TiO_2-rich cumulates is critical to model the compatible behavior of TiO_2 (Fig. 6b). The hornblendite described above, just below the Kohistan arc-MOHO, have whole rock TiO_2 concentration of 2–3 wt%, occasionally up to 6 wt%. These rocks are composed of TiO_2-rich ($\sim$1–2 wt%) hornblende along with Ti-oxides (ilmenite, $\pm$rutile) (Müntener et al. in prep). Fractionation of 10% of these rocks is sufficient in the model to lower the TiO_2 content of the derivative liquids below the concentration measured in gabbroic rocks so that subsequent fractionation of gabbroic cumulates results in the compatible behavior of TiO_2 with or without assimilation (Fig. 6b).

The K/Rb ratio even so highly scattered in the granitoid dataset is dominantly characterized by an initial steep decrease in K/Rb ratio with limited enrichment in Rb concentrations followed by a modest decrease in K/Rb with significant increase in Rb concentration. This trend, exhibited for samples with low K/Rb ratios (<550) is well reproduced by the fractionation model (Fig. 6). The initial decrease in K/Rb with limited Rb enrichments in the model is due to the early appearance of hornblende in the fractionation sequence (e.g., in hornblendite). The magnitude of K/Rb variation is directly related to the interval of hornblendite fractionation. This result conflicts with the general assumption that this initial decrease in K/Rb occurs in composition too primitive to have saturated in a K-rich mineral (e.g., Hildreth and Moorbath 1988).

In the Kohistan, New Britain and Aleutian granitoids a second group of samples is present with very high K/Rb (>550) and low Rb concentrations. These high K/Rb ratios cannot be explained by the modeled fractionation trend. If these K/Rb ratios are the result of bulk assimilation of lower crustal rocks (e.g., diorite), they indicate very high degree of assimilation (40–70%) (Fig. 7). However, the high K/Rb ratios do not correlate with other incompatible element concentrations (e.g., Sr, Pb, Hf, Zr) as could be expected for assimilation mechanism. Also there is no systematic relationship between high K/Rb and SiO_2 concentration and rocks with high K/Rb ratios range in SiO_2 composition from 45 to 73 wt%. However, a significant part of the samples with high K/Rb have a positive Eu/Eu* anomaly even at elevated SiO_2 concentrations. Despite that the dataset is still very small and might not yet be representative, rocks with high K/Rb ratio appear to have higher normative plagioclase content (Fig. 7). Therefore, the high K/Rb ratios could

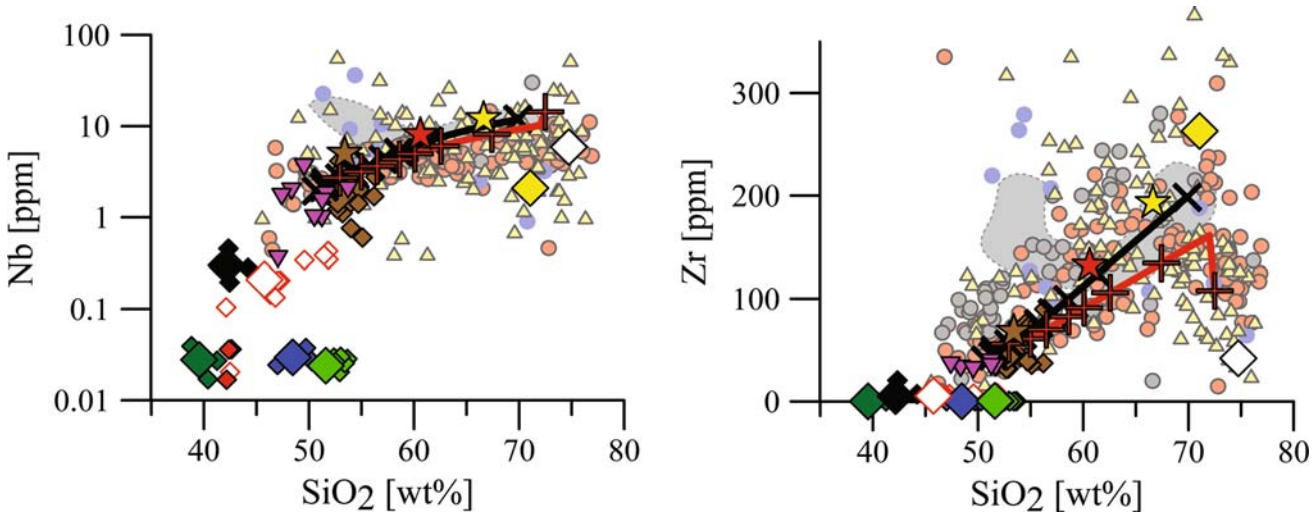

Fig. 8 The Zr and Nb systematic in volcanics from Mt. Jefferson (Conrey et al. 2001) (*gray field*) are considered indicative of intracrustal processes. The distinctive trend of Mt Jefferson volcanics is largely absent in the arc granitoids, which generally follow the fractionation trend

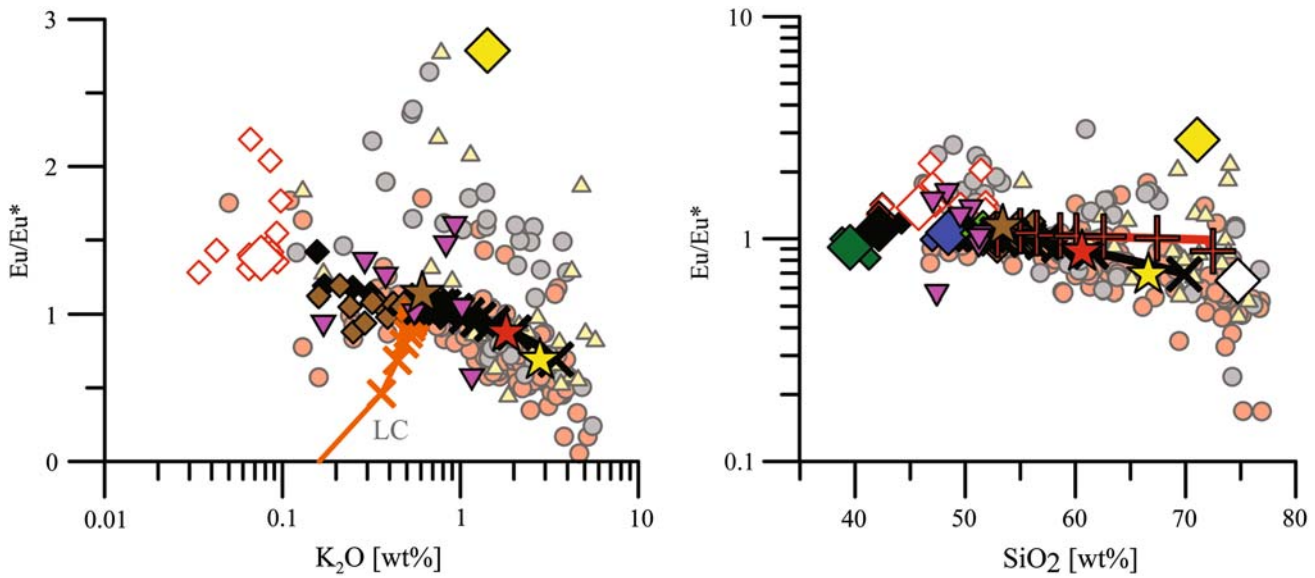

Fig. 9 Eu/Eu* versus K_2O/SiO_2 diagram illustrates the non-complementary lower and upper crustal rock compositions: The trend labeled "*LC*" documents the magma evolution for a primitive parental magma fractionating average lower crustal composition. As the bulk lower crust is too elevated in incompatible elements, this trend is inadequate to explain upper crustal composition. The fractionation trend calculated here is appropriate to produce the average upper crustal composition. (Some fractionated compositions and the assimilation trend are omitted in the plots to preserve clarity)

alternatively be the result of plagioclase accumulation and/or trapped interstitial liquids, also in rocks with elevated SiO_2 concentration (cumulative tonalite). Plagioclase can have K/Rb in the order of 500–3,500 and very low Rb concentration (<0.6 ppm) (Jagoutz et al. 2007). It is noteworthy that rocks with very high K/Rb ratios are absent in the Peninsular Ranges batholith data set (Lee et al. 2007), even in rocks with high $^{87/86}Sr$ isotopic composition as could be expected if high K/Rb ratios are solely due to assimilation processes. Also samples from the Sierra Nevada batholith have no pronounced positive Eu/Eu* at elevated SiO_2 concentrations (i.e., no cumulative tonalite?).

In the fractionation model the Zr and Nb concentration, in accordance with the dominant trend observed in the arc granitoids increase with the SiO_2 concentration. The trend for assimilation is not significantly different from the pure fractionation trend and differs significantly from the Zr and Nb versus SiO_2 trend observed in Mount Jefferson Cascades, which has been attributed to magma mixing processes (Conrey et al. 2001) (Fig. 8).

The bulk lower crust is estimated to have basaltic incompatible element concentration and only a slightly pronounced positive Eu/Eu* anomaly, inadequate to complement upper crust composition (Fig. 9). The fractionation model successfully reproduces the K/(Eu/Eu*) of the upper crust. The primitive garnet and/or hornblende-bearing gabbroic rocks have a pronounced positive Eu/Eu* anomaly and low incompatible element concentration adequate to balance the negative Eu/Eu* anomaly and the incompatible element-enriched nature of the upper crust (Fig. 9). The compositions found in the lower part of the Kohistan arc are appropriate to produce the upper continental crust. However, the reproduced trend is inadequate to reproduce the bulk continental crust composition. In general, the arc granitoids and the modeled trend have a too low Mg# at a given SiO_2 concentration in comparison with the bulk continental crust (Fig. 4), and the bulk sub-Moho composition of the model is basaltic-andesitic in composition (melt composition after 30% fractionation Table 1). This indicates that the accepted bulk continental crust composition can only be explained by additional non-comagmatic process. If the inferred processes modeled in this paper are important crust-forming mechanisms, significant delamination of the low-silica gabbroic rock must occur in order to counterbalance the andesitic composition of the bulk crust.

Role of the parental magma composition

The parental liquid composition is a major controlling parameter in a pure fractional crystallization model. Isotopic data indicate that the Kohistan sequence is not formed from a single parental magma composition. Primitive mantle-derived melts in subduction zones show a significant spread in major element composition, especially in initial SiO_2 content (Grove et al. 2003), which is crucial to explain the silica-rich upper crustal compositions. Therefore, it is likely that a variety of primitive magma compositions are responsible for the formation of the Kohistan arc. Few primitive arc magmas are reported from Kohistan, and those are dominantly basaltic to basaltic-andesitic in composition, but a single analysis of a primitive magnesian andesite exists (Bignold et al. 2006). If the currently available dataset is representative, it indicates that the Kohistan arc was dominantly formed from primitive arc basalts and basaltic-andesites. Based on the results of the fractionation model it seems unlikely that high-alumina olivine tholeiites (HAOT) are an important parental magma composition for the Kohistan arc granitoids as they are too rich in Al_2O_3 to be suitable parental magma for the investigated arc granitoids. It was not possible to model the granitoid dataset using realistic Kohistan cumulate composition and volumes and a HAOT parental melt. As the spread in silica concentration is appreciable in potential Kohistan parental melts, the relative importance of parental magma composition and assimilation to produce the SiO_2 concentration of the upper continental crust might vary. Yet, experiments document that initial difference in parental liquid composition decrease with advancing degree of fractionation largely due to different proportions of ultramafic cumulates (Kägi 2000). In general, the here assumed 30% ultramafic cumulates fractionated below the MOHO are towards the lower conservative end considered realistic. Silica-poorer magmas likely fractionate larger volumes of ultramafic rocks, which might enhance the silica enrichment of derivative liquids and so reduce the required assimilation in the lower crust.

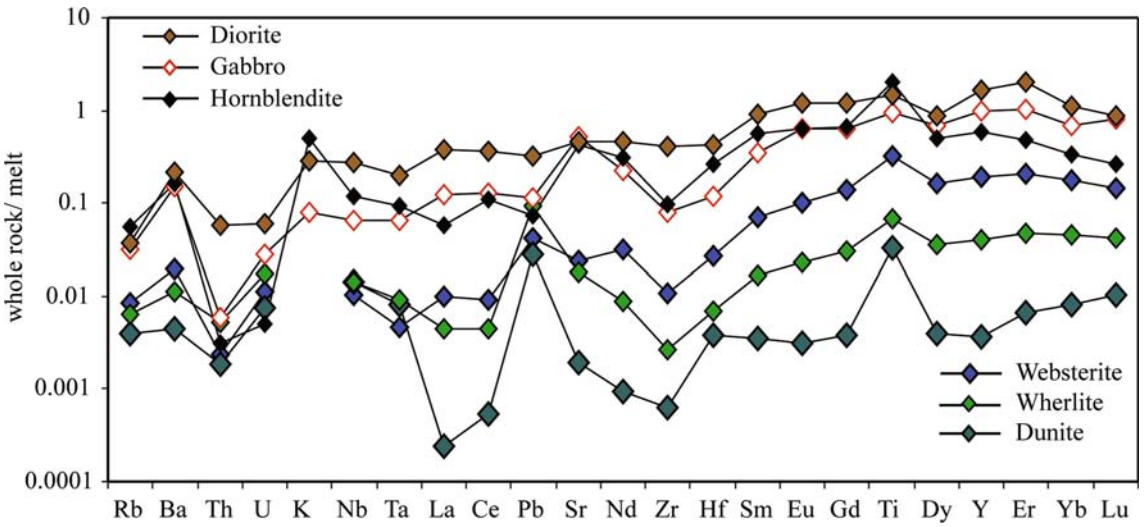

Fig. 10 Modeled apparent bulk partition coefficients between the fractionated composition and the melt composition during the corresponding fractionation step

Discussion

Comparison with standard least square fractionation models

The question is whether the separated cumulate compositions are consistent with generally accepted trace element distribution coefficients and the rock modes. In Fig. 10, calculated apparent bulk partition coefficients (K_D's) are presented by dividing the cumulates by the respective modeled melts. Most of the apparent partitioning is consistent with what would be expected from mineral-melt K_D's, but there are some features needing further consideration and explanation. A strong positive partitioning anomaly for K in the hornblendite (0.5) and the diorite (0.3), and less for the gabbro (0.08) is observed. The observed hornblende K_D is not surprising as hornblende K_D's are typically in the range of 0.3–0.5, but the diorite has only ~30% modal amphibole; yet it is the high K_D that allows the hornblendite and the diorite to reduce the K/Rb of derivative melts. Least-square calculations of a mode for the diorite using calcic-intermediate plagioclase, two pyroxenes, oxides, and hornblende K_D's (using intermediate compositions) only poorly reproduce the diorite K_D's unless biotite and evolved (granitic) trapped melt are included. This indicates that the proposed cumulates are not simple orthocumulates but more complex rocks with trapped melt and minerals (biotite) likely produced by circulating intercumulus liquids.

A strong spike for Pb partitioning is observed in the dunite and the wherlite and to a lesser extent in the websterite. The major mineral phases in the rock (olivine pyroxene and spinel) typically have too low Pb concentration to accommodate such high Pb concentrations (own unpublished data). Likely the high Pb concentration are due to sulfide-bearing phases that are common in the ultramafic cumulates of the Kohistan arc (Miller et al. 1991; Jagoutz et al. 2007) and might indicate that magmas were sulfide-saturated at deep levels.

Uncertainty of the model

There are important uncertainties associated with the model that need to be addressed to evaluate the robustness of the conclusion drawn from the model. As mentioned earlier, the residual mantle is not exposed in the studied section, so the total amount of ultramafic material fractionated cannot be constrained from the field and therefore has been chosen based on the Mg# evolution of the melt and generally accepted values. The total amount of ultramafic cumulate volumes depends on parental magma composition, mean pressure of fractionation etc. and can vary substantially. The 30% chosen in the model presented is, however, towards the lower, more conservative end. Fractionating larger volumes of ultramafite below the MOHO will enhance the silica-enrichment of derivative liquids supporting the main conclusion of the model that fractional crystallization is the crucial mechanism to produce the Kohistan granitoids. A major result of the model is that the fractionation of hornblendite rocks, composed of amphibole and Fe-oxide is essential, particularly to lower the TiO_2 and increase the SiO_2 concentrations of supra-MOHO magmas. This comes about because the parent magma and 30% ultramafic crystallization produce a daughter liquid with SiO_2 and TiO_2, very similar to the gabbro and diorite composition. Potential parent magmas in Kohistan have an appreciable range in SiO_2 and TiO_2. One could envision that the dominant arc parental melt in Kohistan generally contains lower TiO_2 or/and is silica-richer than the melt chosen here (e.g., more towards boninitic compositions) in which case the fractionation of the hornblendite is not required. Such compositions are rare in the Kohistan arc, yet described. Bignold et al. (2006) describe two primitive boninitic rocks from the Chalt group, yet those rocks have rather low Ni (65 ppm) or Cr (72 ppm) content to be true primitive mantle-derived melts and therefore were omitted from the parental magma calculation. Alternatively, one might envision that the gabbroic or dioritic rocks have higher TiO_2 content than the rocks used in this model. The composition used is already slightly towards the upper end in terms of TiO_2 of the composition present in the Southern Plutonic Complex. Higher TiO_2 concentration in gabbroic to dioritic rocks is only found in the magnetite-bearing gabbros of the Chilas Complex, where amphibole occurs as a late magmatic phase (Jagoutz et al. 2007). Those rocks are, however, inappropriate complements for the Kohistan batholith in terms of their incompatible elements concentrations.

A significant uncertainty concerns the average composition used for a given fractionated composition. Even though all compositions are within the range of composition of the appropriate rocks found in the field, it is difficult to evaluate how volumetrically representative the analyzed rocks are. For example, a significant range in composition is observed for the gabbroic rocks (indicated by the 2 sigma variability of the averaged composition; Table 1), yet it is difficult to relate the variable composition to volumes. Given the limited dataset available, it is possible that a volumetrically important composition is only represented by a single sample and thereby strongly underrepresented in any average. Ideally, an averaged composition that reflects the different volumes of the variable compositions of the single unit in the field should be used for a model such as the one presented here. Our current knowledge of the geology of Kohistan is, however, inadequate to address those issues.

Implications

The model shows that fractional crystallization in combination with assimilation of few percent of crustal melt can reproduce the dominant trends measured in arc granitoids. The preserved succession of dunite, wherlite, websterite, garnetite/hornblendite gabbro, diorite, tonalite from south to north, i.e., from deeper to shallower levels of the crust in Kohistan is adequate to explain the geochemical trend of arc granitoids for essentially all major and trace elements considered in this study. Even complex non-linear behavior of, e.g., SiO_2 versus Mg# (Fig. 4) can be explained by the fractionated cumulate composition and sequence. The highly variable Mg# at nearly constant high SiO_2 concentration, which has been explained by partial melting processes (e.g., Lee et al. 2007), is in the model essentially the result of the low concentration of MgO in evolved rocks. Slight variations in MgO are amplified in the Mg#.

The fact that the rock sequence preserved is adequate to explain the observed trends in arc granitoids is in accord with the idea that the rocks in the ultramafic cumulate 'mantle' part of the Kohistan arc are related to the mafic 'crustal' part by a common formation mechanism (Müntener et al. 2001). Based on a postulated Mg# gap and isotopic difference between 'mantle' rocks and the 'crust' of the Kohistan, it has been postulated that the Jijal ultramafite are genetically unrelated to the crustal rocks (Dhuime et al. 2007). The model presented here documents that fractionation of the observed relative volumes and composition is adequate to explain the Mg# evolution of the Kohistan granitoids, and no evidence for missing cumulate fractions or for the proposed Mg# gap is observed. Yet, age constraint and isotopic studies indicate that the Southern Plutonic Complex was formed over an extended time period (Yamamoto and Nakamura 1996, 2000; Schaltegger et al. 2002; Yamamoto et al. 2005) and from isotopically distinctive melts (Dhuime et al. 2007, 2009).

Trace element characteristics indicating that appreciable amounts of crustal melting or assimilation has taken place to produce intermediate and evolved magma compositions are generally absent in the arc granitoid dataset used. Instead, the fractionation of silica-poor minerals like amphibole, garnet, and anorthite-rich plagioclase is crucial to explain the documented trends. The stability of those minerals is enhanced by elevated water and confining pressures (Yoder and Tilley 1962; Green and Ringwood 1968; Alonso-Perez et al. 2009).

The importance of amphibole and plagioclase fractionation in Kohistan arc granitoids is made evident by the ubiquitous occurrence of those phases in the lower part of the Kohistan arc. This observation, together with geochemical data such as the compatible behavior of TiO_2 during SiO_2-enrichment implies that amphibole was present in the fractionation sequence over a significant interval. Even if amphibole is often absent in volcanic arc rocks, it is common in plutonic xenoliths from various subduction zones (Arculus and Wills 1980) and has been inferred to be an important mineral for arc magma evolution based on geochemical arguments (Davidson et al. 2007).

The role of garnet in the fractionation sequence is less clear. In terms of major element composition, both fractionation of garnet or amphibole are adequate to produce upper continental crust compositions and volumes if the onset of amphibole or garnet fractionation occurs early in the fractionation sequence (i.e., before plagioclase, see later). Accordingly, hydrous high-pressure fractionation involving garnet at pressure >0.8 GPa in basaltic to andesitic compositions (Alonso-Perez et al. 2009) is not a necessary premise for silica-enrichment. Similar silica-enrichment can be achieved by moderate pressure fractionation invoking amphibole, oxides, and anorthite-rich plagioclase (Sisson et al. 2005). Obviously, fractionation of garnet or hornblende will be imprinted on the evolution of the HRE elements during silica enrichment. The garnetites present below the Moho in Kohistan have a strong HREE enrichment indicating magmatic accumulation of garnet. Significant garnet fractionation will result in an indifferent

Table 2 Compilation of the SiO_2 versus Yb relationship in whole rocks for different arcs

Arc	Crustal thickness (km)	Yb concentration (ppm)		Variability[a] (1σ)	N[b]
		50 wt% SiO_2	66 wt% SiO_2		
Cascades	45	1.9	1.6	0.46	672
Aleutian	30	2.3	2.6	0.79	467
Vanuatu	28	1.9	4.2	0.64	387
Ryuku	25	2.4	3.2	0.87	181
Marianna	17	2.4	4.1	0.67	279
Central America	42	1.8	2.1	0.45	539
New Zealand	36	2.0	2.3	0.77	473
Kermadec	18	1.9	3.7	0.59	73
Kurille	23	2.6	2.9	0.62	175
Tonga	12	2.3	3.5	1.07	463
Southern Volcanic Zone	30	2.1	2.0	0.69	899
Central Volcanic Zone	50	1.9	1.7	0.46	989
TTG	?	1.7	1.0	0.44	162

Crustal thicknesses are from (Gill 1981; Stern 1991; Beck et al. 1996; Shillington et al. 2004)

[a] Variability is the standard deviation of the residuals

[b] Number of analyses in the dataset

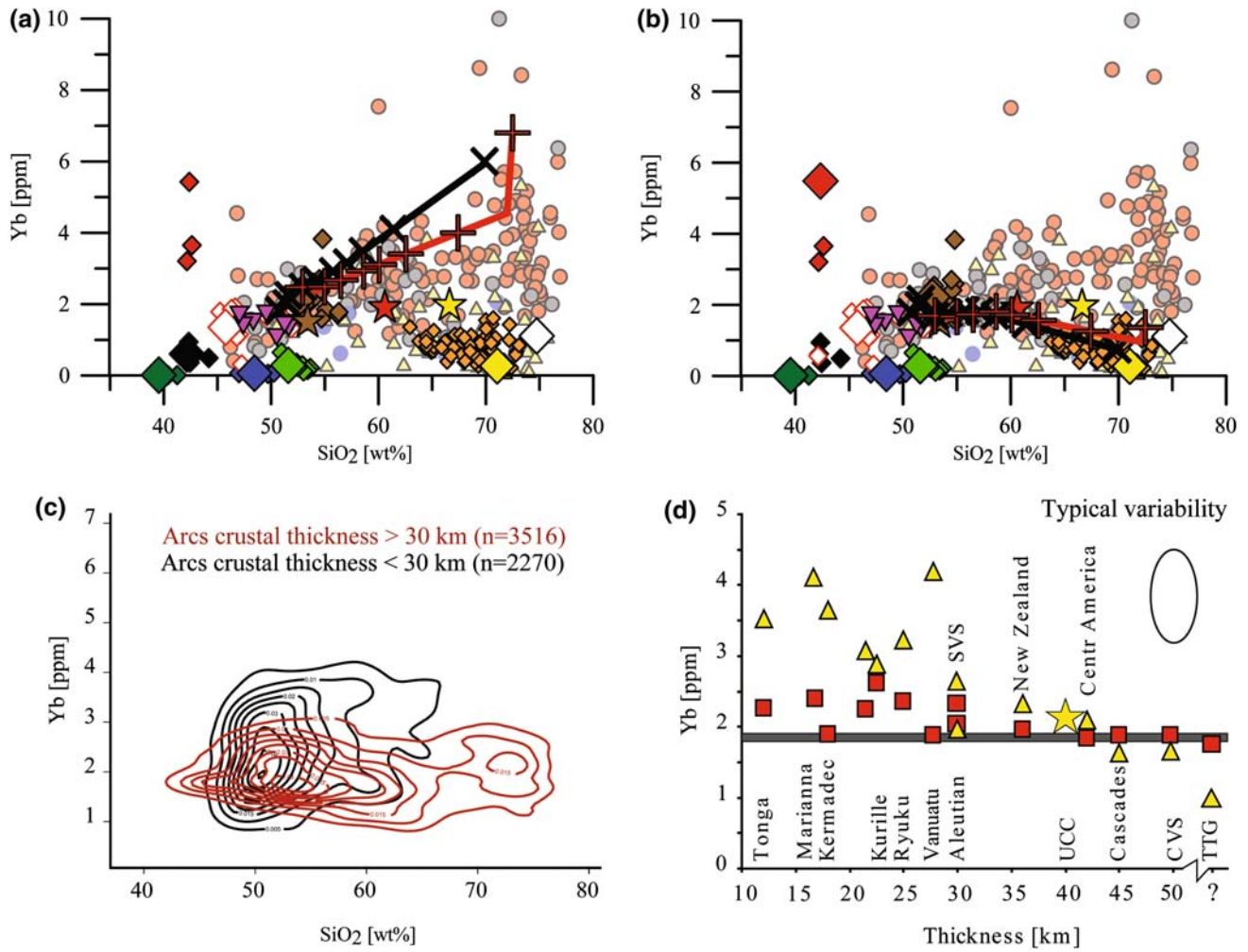

Fig. 11 Illustration of the behavior of Yb during the fractionation sequence depending on the presence or absence of magmatic garnet in the fractionation sequence. **a** Hornblende dominated fractionation results in an overall incompatible Yb behavior with increasing SiO_2 content. **b** Alternatively, the fractionation of 10% magmatic garnetite present at the base of the Kohistan arc results in an overall incompatible behavior of Yb. The Kohistan arc granitoids preserve both trends. **c** Global correlation of the dependence of Yb behavior with increasing SiO_2 content. Thick arcs (>30 km) have significantly different SiO_2 versus Yb relationship than thinner arcs. [Contoured plot in percentage, done with GCDKit 2.3 (Janousek et al. 2006)] **d** Yb concentration at 50 and 66 wt% silica concentration (*red squares* and *yellow triangles*, respectively) for the fractionation trends observed in different arcs. The Yb concentration at low silica concentration is similar in all arcs (within the observed variability) and independent from the crustal thickness. The Yb concentration of high silica rocks varies nonlinear with crustal thickness. The transition between incompatible and compatible behavior occurs at ~25–30 km and coincides with the experimentally determined appearance of magmatic garnet in hydrous basaltic to andesitic compositions (~8 kbar Müntener et al. 2001)

or even compatible behavior of the HREE with increasing SiO_2 enrichment. On the contrary, hornblende- and plagioclase-dominated fractionation produces an overall incompatible behavior of the HREE. To illustrate the effect of garnet fractionation, a model is presented where the garnetite composition was used instead of hornblendite (Fig. 11). Garnet fractionation produces granitoids with low HREE concentration similar to Archean TTG rocks (Condie 2008), whereas hornblende fractionation produces granitoids with higher HREE concentrations. Granitoids in Kohistan follow both the higher-pressure "garnet" trend and the moderate-pressure "hornblende" trend. Currently, no constrains exist on the relative importance of the different fractionation trends in terms of volume of crust produced in Kohistan or age relation between both.

To understand the global importance of the garnet and amphibole fractionation, I compiled a whole rock data set from the GEOROC database (http://georoc.mpch-mainz.gwdg.de/georoc/) and studied the SiO_2 versus Yb relationship for a variety of magmatic arcs. I calculated the trend for SiO_2 versus Yb for each arc studied and the residual of the scatter around the trend (Table 2). Even though there is

significant scatter in single datasets (documented by the standard deviation of the residuals), the average Yb concentration for basaltic rocks (i.e., at $SiO_2 = 50$ wt%) is similar in all arcs (Table 2; Fig. 11). However, two groups of arcs can be separated based on the Yb versus SiO_2 relationship for silica-rich rocks (Fig. 11). For that I calculated a linear fit to the data and through the regression approximate the Yb concentration of the various arcs at average upper crustal SiO_2 concentration ($\sim$66 wt%). In some arcs Yb behaves incompatible, and evolved rocks have Yb concentration higher than the corresponding basaltic rocks, whereas in other arcs Yb is indifferent or compatible and evolved rocks have lower or equal Yb concentrations compared with the corresponding basalts (Fig. 11; Table 2). The in- or compatible behavior of Yb correlates non-linear with crustal thickness. In arcs with a crustal thickness <30 km, Yb behaves incompatible, whereas in arcs with a crustal thickness of >30 km Yb is indifferent or compatible. The transition coincides with the pressure range of the garnet-in phase boundary in basaltic to andesitic melts (>8 kbar) (Müntener et al. 2001; Alonso-Perez et al. 2009). Accordingly, the intracrustal evolution of thin arcs is dominated by the incompatible "hornblende" trend, whereas in thicker arcs (i.e., $\geq$30 km) intracrustal processes include garnet. Archean TTG gneisses have comparable SiO_2–Yb relations as thick arcs (Fig. 11). This observation stresses the importance of garnet as a magmatic phase in intracrustal process and has to be taken in consideration when relating a "garnet" signature to a certain source of the melt (e.g., slab melt etc.).

Importance of amphibole fractionation in the Kohistan arc

The suggestion that amphibole-controlled fractionation produces silica-rich derivative liquids is of old vintage (Daly 1933) and has recently been reemphasized (Davidson et al. 2007). Yet it is often assumed the amphibole is a liquidus phase only in more evolved intermediate compositions. The presence of massive volumes of magmatic amphibole in rather primitive rocks (Mg# $\sim$0.6–0.7) in Kohistan indicates that amphibole can be a liquidus phase also in more primitive compositions. The textural relationships of amphibole with other rock-forming minerals point to two separate fractionation sequences in the Kohistan mafic rocks: amphibole with high Mg# precedes plagioclase in the fractionation sequence in the Jijal Complex; it is the contrary in the Chilas Complex and amphibole (Jagoutz et al. 2007). Experimental evidences indicate that higher initial water content and/or ambient pressure stabilizes amphibole in respect to plagioclase (Sisson and Grove 1993; Grove et al. 2003). However, the exact details of amphibole appearance in the fractionation sequence are ill understood and also controlled by the bulk magma chemistry (e.g., Ca/Na, $Mg\#_{melt}$), the f_{O2} and silica activity (e.g., Heltz 1982). As most of these parameters are poorly constrained in the Kohistan arc, I speculate that the difference between the two fractionation sequences is related to different initial water contents and/or ambient pressures. As I have shown earlier, the early appearance of amphibole in the fractionation sequence is crucial to produce upper continental crust, I conclude that upper crustal granitoids in Kohistan are dominantly derived from hydrous basaltic parental magmas. This idea is consistent with the evolution trend in arc granitoids necessitating a parental melt with a relatively low Al_2O_3 content. It has been shown that subduction-zone-related primitive basalt and basaltic-andesite are more hydrous than HAOT (Grove et al. 2002). Grove and co-workers (Grove et al. 2002, 2003), related these different magma compositions to different melting mechanisms: flux melting produces "more" hydrous basalt and basaltic andesite, whereas "less" hydrous HAOT result from decompression melting. Following this argument, I speculate that the Si-rich upper continental arc crust is formed from hydrous, mantle-derived melts formed by flux melting. These melts evolve dominantly through fractional crystallization in the middle to lower part of the crust in combination with minor assimilation of crustal melts to produce silica-rich rocks, similar in composition to the upper continental crust.

Conclusion

Simple model calculation using actual cumulate composition found in the Kohistan arc document that moderate- to high-pressure fractional crystallization associated with minor amounts of assimilation could produce upper continental crust. The lower part of the Southern Plutonic Complex is complementary to the Kohistan batholith. Hornblendite and garnetite found at the base of the Kohistan arc are crucial units to explain silica enrichment and the behavior of certain elements in Kohistan granitoids and other arcs.

The rocks preserved in the Southern Plutonic Complex are unique to the exposed rock record. Comparable rock compositions are only described from xenolith suites (e.g., Horodyskyj et al. 2007). Density measurements indicate that the large part of the sequence has higher densities than typical mantle harzburgite; this includes the pyroxenites, garnet hornblendites and some of the garnet gabbros (Miller and Christensen 1994). Those rocks had the potential to delaminate in geological timescales and sink back into the mantle (Jull and Kelemen 2001). Accordingly, the lower part of the Southern Plutonic Complex is a preserved example of the normally delaminated (?) lower

crust that is compositionally complimentary to the upper crust. Clearly, the obsolute volumes of expose rock are inadequate to complement the observed volumes of the Kohistan batholith. It is likely that the majority of the complementary compositions delaminated, whereas the question why those rocks in the Southern Plutonic Sequence are preserved and did not delaminate remains.

Acknowledgments Discussions with Matt Rioux, Tim Grove and Othmar Müntener helped to shape these ideas. Bruno Dhuime is thanked for sharing in-depth details related to his geochemical dataset. Othmar Müntener is thanked for comments on the manuscript and the very helpful, detailed, and thoughtful journal reviews by Tom Sisson and an anonymous reviewer greatly improved the manuscript.

References

Alonso-Perez R, Müntener O, Ulmer P (2009) Igneous garnet and amphibole fractionation in the roots of island arcs: experimental constraints on H_2O undersaturated andesitic liquids. Contrib Mineral Petrol 157:541–558

Annen C, Blundy JD, Sparks RSJ (2006) The genesis of intermediate and silicic magmas in deep crustal hot zones. J Petrol 47:505–539

Arbaret L, Burg JP, Zeilinger G, Chaudhry N, Hussain S, Dawood H (2000) Pre-collisional anastomosing shear zones in the Kohistan Arc, NW Pakistan. In: Khan MA, Treloar Peter J, Searle Michael P, Jan MQ (eds) Tectonics of the Nanga Parbat syntaxis and the western Himalaya. Geological Society of London, London

Arculus RJ, Wills KJA (1980) The petrology of plutonic blocks and inclusions from the Lesser Antilles island arc. J Petrol 21:743–799

Bard JP (1983) Metamorphism of an obducted island arc; example of the Kohistan Sequence (Pakistan) in the Himalayan collided range. Earth Planet Sci Lett 65:133–144

Beck SL, Zandt G, Myers SC, Wallace TC, Silver PG, Drake L (1996) Crustal-thickness variations in the central Andes. Geology 24:407–410

Bignold SM, Treloar PJ (2003) Northward subduction of the Indian Plate beneath the Kohistan island arc, Pakistan Himalaya: new evidence from isotopic data. J Geol Soc 160:377–384

Bignold SA, Treloar PJ, Petford N (2006) Changing sources of magma generation beneath intra-oceanic island arcs: an insight from the juvenile Kohistan island arc, Pakistan Himalaya. Chem Geol 233:46–74

Bowen NL (1928) The evolution of the igneous rocks. Dover Publications, Inc, New York

Burg JP, Arbaret L, Chaudhry NM, Dawood H, Hussain S, Zeilinger G (2005) Shear strain localization from the upper mantle to the middle crust of the Kohistan Arc (Pakistan). In: Bruhn D, Burlini L (eds) High-strain zones: structure and physical properties, vol 245, Special Publications. Geological Society, London, pp 25–38

Burg JP, Jagoutz O, Hamid D, Hussain S (2006) Pre-collision tilt of crustal blocks in rifted island arcs: structural evidence from the Kohistan Arc. Tectonics 25:13. doi:10.1029/2005TC001835

Clemens JD, Vielzeuf D (1987) Constraints on melting and magma production in the crust. Earth Planet Sci Lett 86:287–306

Condie KC (2008) Did the character of subduction change at the end of the Archean? Constraints from convergent-margin granitoids. Geology 36:611–614

Conrey RM, Hooper PR, Larson PB, Chesley J, Ruiz J (2001) Trace element and isotopic evidence for two types of crustal melting beneath a High Cascade volcanic center, Mt. Jefferson, Oregon. Contrib Mineral Petrol 141:710–732

Coward MP, Windley BF, Broughton RD, Luff IW, Petterson MG, Pudsey CJ, Rex DC, Asif KM (1986) Collision tectonics in the NW Himalayas. In: Coward MP, Ries Alison C (eds) Collision tectonics, vol 19. Geological Society Special Publications, London, United Kingdom, Geological Society of London, pp 203–219

Coward MP, Butler RWH, Asif KM, Knipe RJ (1987) The tectonic history of Kohistan and its implications for Himalayan structure. J Geol Soc Lond 144:377–391

Daly RA (1933) Igneous rocks and the depth of the Earth. McGraw-Hill, New York

Davidson J, Turner S, Handley H, Macpherson C, Dosseto A (2007) Amphibole "sponge" in arc crust? Geology 35:787–790

Dhuime B, Bosch D, Bodinier JL, Garrido CJ, Bruguier O, Hussain SS, Dawood, H (2007) Multistage evolution of the Jijal ultramafic-mafic complex (Kohistan, N Pakistan): implications for building the roots of island arcs. Earth Planet Sci Lett. doi:10.1016/j.epsl.2007.06.026

Dhuime B, Bosch D, Garrido CJ, Bodinier JL, Bruguier O, Hussain SS, Dawood H (2009) Geochemical architecture of the lower- to middle-crustal section of a Paleo-island Arc (Kohistan Complex, JijalKamila Area, Northern Pakistan): implications for the evolution of an oceanic subduction zone. J Petrol 50:531–569

Dufek J, Bergantz GW (2005) Lower crustal magma genesis and preservation: a stochastic framework for the evaluation of the basalt–crust interaction. J Petrol 46:2167–2195

Eiler JM, Crawford A, Elliott T, Farley KA, Valley JW, Stolper EM (2000) Oxygen isotope geochemistry of oceanic-arc lavas. J Petrol 41:229–256

Eiler JM, Schiano P, Valley JW, Kita NT, Stolper EM (2007) Oxygen-isotope and trace element constraints on the origins of silica-rich melts in the subarc mantle. Geochem Geophys Geosyst 8:Q09012. doi:10.1029/2006GC001503

Enggist A (2007) Geobarometry and magmatic processes. Kohistan Batholith, Pakistan

Garrido CJ, Bodinier JL, Burg JP, Zeilinger G, Hussain SS, Dawood H, Chaudhry MN, Gervilla F (2006) Petrogenesis of mafic garnet granulite in the lower crust of the Kohistan paleo-arc complex (northern Pakistan); implications for intra-crustal differentiation of island arcs and generation of continental crust. J Petrol 47:1873–1914

Gill J (1981) Orogenic andesites and plate tectonics. Springer, Berlin, p 390

Green TH, Ringwood AE (1968) Genesis of the calcalkaline igneous suite. Contrib Mineral Petrol 18:105–162

Greene AR, DeBari SM, Kelemen P, Blusztajn JS, Clift Peter D (2006) A detailed geochemical study of island arc crust: the Talkeetna Arc Section, South-Central Alaska. J Petrol 47:1051–1093

Grove TL, Parman SW, Bowring SA, Price RC, Baker MB (2002) The role of an H_2O-rich fluid component in the generation of primitive basaltic andesites and andesites from the Mt. Shasta region, N California. Contrib Mineral Petrol 142:375–396

Grove TL, Elkins-Tanton LT, Parman SW, Chatterjee N, Muntener O, Gaetani GA (2003) Fractional crystallization and mantle-melting controls on calc-alkaline differentiation trends. Contrib Mineral Petrol 145:515–533

Hacker BR, Mehl L, Kelemen PB, Rioux M, Behn MD, Luffi P (2008) Reconstruction of the Talkeetna intraoceanic arc of Alaska through thermobarometry. J Geophys Res 113:B03204. doi:10.1029/2007JB005208

Harley SL (1989) The origins of granulites—a metamorphic perspective. Geol Mag 126:215–247

Hawkesworth CJ, Kemp AIS (2006) The differentiation and rates of generation of the continental crust. Chem Geol 226:134–143

Heltz RT (1982) Phase relations and composition of amphiboles produced in studies of the melting behavior of rocks. In: Veblen

DR, Ribbe PH (eds) Petrology and experimental phase relations, vol 9B. Mineralogical Society of America, Virginia, pp 279–354
Hildreth W, Moorbath S (1988) Crustal contributions to arc magmatism in the Andes of Central Chile. Contrib Mineral Petrol 98:455–489
Horodyskyj UN, Lee CTA, Ducea MN (2007) Similarities between Archean high MgO eclogites and Phanerozoic arc-eclogite cumulates and the role of arcs in Archean continent formation. Earth Planet Sci Lett 256:510–520
Huppert HE, Sparks RSJ (1988) The generation of granitic magmas by intrusion of basalt into continental-crust. J Petrol 29:599–624
Jagoutz O, Müntener O, Burg J-P, Ulmer P, Jagoutz E (2006) Lower continental crust formation through focused flow in km-scale melt conduits: the zoned ultramafic bodies of the Chilas Complex in the Kohistan Island arc (NW Pakistan). Earth Planet Sci Lett 242:320–342
Jagoutz O, Müntener O, Ulmer P, Burg J-P, Pettke T (2007) Petrology and mineral chemistry of lower crustal intrusions: the Chilas Complex, Kohistan (NW Pakistan). J Petrol 48:1895–1953
Jagoutz O, Burg J-P, Hussain S, Dawood H, Pettke T, Iizuka T, Maruyama S (2009) Construction of the granitoid crust of an island arc part I: geochronological and geochemical constraints from the plutonic Kohistan (NW Pakistan). Contrib Mineral Petrol 158:739–755
Jan MQ, Howie RA (1981) The mineralogy and geochemistry of the metamorphosed basic and ultrabasic rocks of the Jijal Complex, Kohistan, NW Pakistan. J Petrol 22:85–126
Jan MQ, Windley BF (1990) Chromian spinel-silicate chemistry in ultramafic rocks of the Jijal Complex Northwest Pakistan. J Petrol 31:667–715
Janousek V, Farrow CM, Erban V (2006) Interpretation of whole-rock geochemical data in igneous geochemistry: introducing geochemical data toolkit (GCDkit). J Petrol 47:1255–1259
Jull M, Kelemen PB (2001) On the conditions for lower crustal convective instability. J Geophys Res B Solid Earth Planets 106:6423–6446
Kägi R (2000) The liquid line of descent of hydrous. Primary, calc-alkaline magmas under elevated pressure. An experimental approach. Zürich
Kay SM, Kay RW (1985) Role of crystal cumulates and the oceanic crust in the formation of the lower crust of the Aleutian arc. Geology 13:461–464
Kay SM, Kay RW, Citron GP, Perfit MR (1990) Calc-alkaline plutonism in the intra-oceanic Aleutian Arc, Alaska. In: Kay SM, Rapela CW (eds) Plutonism from Antarctica to Alaska, vol 241, Geological Society of America Special Paper, pp 233–255
Kelemen PB (1995) Genesis of high Mg andesites and the continental crust. Contrib Mineral Petrol 120:1–19
Kelemen P, Hanghoj K, Greene A (2003a) One view of the geochemistry of subduction-related magmatic arcs, with an emphasis on primitive andesite and lower crust. In: Rudnick RL (ed) The crust, vol 3: treatise on geochemistry. Elsevier–Pergamon, Oxford, pp 593–659
Kelemen P, Rilling JL, Parmentier EM, Mehl L, Hacker BR (2003b) Thermal structure due to solid-state flow in the mantle wedge Beneath Arcs. In: Eiler JM (ed) Inside subduction factory, vol 138: Geophysical Monograph, American Geophysical Union
Kemp AIS, Hawkesworth CJ, Foster GL, Paterson BA, Woodhead JD, Hergt JM, Gray CM, Whitehouse MJ (2007) Magmatic and crustal differentiation history of granitic rocks from Hf-O isotopes in zircon. Science 315:980–983
Khan MA, Jan MQ, Windley BF, Tarney J, Thirlwall MF (1989) The Chilas mafic–ultramafic igneous complex; the root of the Kohistan island arc in the Himalaya of northern Pakistan. In: Malinconico Lawrence L Jr, Lillie Robert J (eds) Tectonics of the western Himalayas, vol 232, Special Paper—Geological Society of America. Geological Society of America (GSA), Boulder, pp 75–94
Khan MA, Jan MQ, Weaver BL (1993) Evolution of the lower arc crust in Kohistan, N. Pakistan; temporal arc magmatism through early, mature and intra-arc rift stages. In: Treloar PJ, Searle MP (eds) Himalayan tectonics, vol 74, Geological Society Special Publications. Geological Society of London, London, pp 123–138
Khan SD, Walker DJ, Hall SA, Burke KC, Shah MT, Stockli L (2008) Did Kohistan-Ladakh island arc collide first with India? Geol Soc Am Bull 121:366–384
Kodaira S, Sato T, Takahashi N, Miura S, Tamura Y, Tatsumi Y, Kaneda Y (2007) New seismological constraints on growth of continental crust in the Izu-Bonin intra-oceanic arc. Geology 35:1031–1034
Lee CTA, Morton DM, Kistler RW, Baird AK (2007) Petrology and tectonics of Phanerozoic continent formation: from island arcs to accretion and continental arc magmatism. Earth Planet Sci Lett 263:370–387
McCulloch MT, Gamble JA (1991) Geochemical and geodynamical constraints on subduction zone magmatism. Earth Planet Sci Lett 102:358–374
Mclennan SM, Taylor SR (1982) Geochemical constraints on the growth of the continental-crust. J Geol 90:347–361
Miller DJ, Christensen NI (1994) Seismic signature and geochemistry of an island arc; a multidisciplinary study of the Kohistan accreted terrane, northern Pakistan. J Geophys Res B Solid Earth Planets 99:11623–11642
Miller DJ, Loucks RR, Ashraf M (1991) Platinum-group element mineralization in the Jijal layered ultramafic-mafic complex, Pakistani Himalayas. Econ Geol (Bull Soc Econ Geol) 86:1093–1102
Morris JD, Leeman WP, Tera F (1990) The subducted component in island arc lavas; constraints from B-Be isotopes and Be systematics. Nature 344:31–36
Müntener O, Ulmer P (2006) Experimentally derived high-pressure cumulates from hydrous arc magmas and consequences for the seismic velocity structure of lower arc crust. Geophys Res Lett 33:L41308. doi:10.1029/2006GL027629
Müntener O, Kelemen PB, Grove TL (2001) The role of H_2O during crystallization of primitive arc magmas under uppermost mantle conditions and genesis of igneous pyroxenites; an experimental study. Contrib Mineral Petrol 141:643–658
Müntener O, Ulmer P, Schmidt MW, Jagoutz O (in prep) Magmatic paragonite and epidote: phase relations and consequences for the igneous evolution of the Kohistan island arc (Pakistan)
Perfit MR, Brueckner H, Lawrence JR, Kay RW (1980) Trace-Element and Isotopic Variations in a Zoned Pluton and Associated Volcanic-Rocks, Unalaska Island, Alaska—a model for fractionation in the Aleutian calcalkaline Suite. Contrib Mineral Petrol 73:69–87
Petterson MG, Windley BF (1985) Rb–Sr dating of the Kohistan arc-batholith in the Trans-Himalaya of North Pakistan, and tectonic implications. Earth Planet Sci Lett 74:45–57
Pitcher WS (1997) The nature and origin of granite. Chapman & Hall, London
Plank T (2005) Constraints from thorium/lanthanum on sediment recycling at subduction zones and the evolution of continents. J Petrol 46:921–944
Pudsey CJ, Coward MP, Luff IW, Shackleton RM, Windley BF, Jan MQ (1985) Collision zone between the Kohistan Arc and the Asian Plate in NW Pakistan: transactions of the Royal Society of Edinburgh. Earth Sci 76:463–479
Ringuette L, Martignole J, Windley BF (1999) Magmatic crystallization, isobaric cooling, and decompression of the garnet-bearing assemblages of the Jijal Sequence (Kohistan Terrane, western Himalayas). Geology (Boulder) 27:139–142

Rudnick RL (1995) Making continental crust. Nature 378:571–578
Rudnick RL, Gao S (2003) The composition of the continental crust. In: Rudnick RL (ed) The crust, vol 3: treatise on Geochemistry. Elsevier, Oxford, pp 1–64
Schaltegger U, Zeilinger G, Frank M, Burg JP (2002) Multiple mantle sources during island arc magmatism; U–Pb and Hf isotopic evidence from the Kohistan arc complex, Pakistan. Terra Nova 14:461–468
Schaltegger U, Heuberger S, Frank M, Fontignie D, Sergeev S, Burg JP (2004) Crust-mantle interaction during Karakoram-Kohistan accretion (NW Pakistan). Goldschmidt 2004. Geochim Cosmochim Acta Copenhagen 68/11
Searle MP, Khan MA, Fraser JE, Gough SJ, Qasim JM (1999) The tectonic evolution of the Kohistan–Karakoram collision belt along the Karakoram Highway transect, North Pakistan. Tectonics 18:929–949
Shah MT, Shervais JW (1999) The Dir-Utror metavolcanic sequence, Kohistan arc terrane, northern Pakistan. J Asian Earth Sci 17:459–475
Shillington DJ, Van Avendonk HJA, Holbrook WS, Kelemen PB, Hornbach MJ (2004) Composition and structure of the central Aleutian island arc from arc-parallel wide-angle seismic data. Geochem Geophys Geosyst 5:Q10006. doi:10.1029/2004GC000715
Sisson TW, Grove TL (1993) Experimental investigations of the role of H (sub 2) O in calc-alkaline differentiation and subduction zone magmatism. Contrib Mineral Petrol 113:143–166
Sisson TW, Ratajeski K, Hankins WB, Glazner AF (2005) Voluminous granitic magmas from common basaltic sources. Contrib Mineral Petrol 148:635–661
Smith DR, Leeman WP (1987) Petrogenesis of Mount St-Helens dacitic magmas. J Geophys Res Solid Earth Planets 92:10313–10334
Stern CR (1991) Role of subduction erosion in the generation of Andean magmas. Geology 19:78–81
Suyehiro K, Takahashi N, Ariie Y, Yokoi Y, Hino R, Shinohara M, Kanazawa T, Hirata N, Tokuyama H, Taira A (1996) Continental crust, crustal underplating, and low-Q upper mantle beneath an oceanic island arc. Science 272:390–392
Tahirkheli RAK, Mattauer M, Proust F, Tapponnier P (1979) The India-Eurasia suture zone in northern Pakistan; synthesis and interpretation of recent data at plate scale. In: Abul F, DeJong KA (eds) Geodynamics of Pakistan. Geological Survey of Pakistan, Quetta, pp 125–130
Taylor SR (1977) Island arc models and the composition of the continental crust. In: Talwani M, Pitman WC III (eds) Island arcs, deep sea trenches and back-arc basins, vol 1, Maurice Ewing Series. American Geophysical Union, Washington, pp 325–335
Taylor SR, Mclennan SM (1981) The composition and evolution of the continental-crust—rare-earth element evidence from sedimentary-rocks. Phil Trans R Soc Lond Ser A Math Phys Eng Sci 301:381–399
Treloar PJ, Petterson MG, Jan MQ, Sullivan MA (1996) A re-evaluation of the stratigraphy and evolution of the Kohistan Arc sequence, Pakistan Himalaya; implications for magmatic and tectonic arc-building processes. J Geol Soc London 153(5):681–693
Tuttle OF, Bowen NL (1958) Origin of granite in the light of experimental studies in the system $NaAlSi_3O_8$–$KAlSi_3O_8$–SiO_2–H2O. Geol Soc Am Mem 74, 153 pp
Vielzeuf D, Schmidt MW (2001) Melting relations in hydrous systems revisited: application to metapelites, metagreywackes and metabasalts. Contrib Mineral Petrol 141:251–267
Whalen JB (1985) Geochemistry of an island-arc plutonic suite; the Uasilau-Yau Yau intrusive complex, New Britain, PNG. J Petrol 26:603–632
White A, Chapell B (1983) Granitoid types and their distribution in the Lachlan Fold Belt, southeastern Australia. Geol Soc Am Mem 159:21–34
Yamamoto H (1993) Contrasting metamorphic *P–T*–time paths of the Kohistan granulites and tectonics of the western Himalayas. J Geol Soc Lond 150(5):843–856
Yamamoto H, Nakamura E (1996) Sm–Nd dating of garnet granulites from the Kohistan Complex, northern Pakistan. J Geol Soc Lond 153(6):965–969
Yamamoto H, Nakamura E (2000) Timing of magmatic and metamorphic events in the Jijal Complex of the Kohistan Arc deduced from Sm-Nd dating of mafic granulites. In: Khan MA, Treloar Peter J, Searle Michael P, Jan MQ (eds) Tectonics of the Nanga Parbat syntaxis and the western Himalaya. Geological Society of London, London
Yamamoto H, Yoshino T (1998) Superposition of replacements in the mafic granulites of the Jijal Complex of the Kohistan Arc, northern Pakistan; dehydration and rehydration within deep arc crust. Lithos 43:219–234
Yamamoto H, Kobayashi K, Nakamura E, Kaneko Y, Kausar Allah B (2005) U–Pb zircon dating of regional deformation in the lower crust of the Kohistan Arc. Int Geol Rev 47:1035–1047
Yoder HS Jr, Tilley CE (1962) Origin of basalt magmas; an experimental study of natural and synthetic rock systems. J Petrol 3:342–529
Yoshino T, Okudaira T (2004) Crustal growth by magmatic accretion constrained by metamorphic *P–T* paths and thermal models of the Kohistan Arc, NW Himalayas. J Petrol 45:2287–2302
Yoshino T, Satish KM (2001) Origin of scapolite in deep-seated metagabbros of the Kohistan Arc, NW Himalayas. Contrib Mineral Petrol 140:511–531
Yoshino T, Yamamoto H, Okudaira T, Toriumi M (1998) Crustal thickening of the lower crust of the Kohistan Arc (N. Pakistan) deduced from Al zoning in clinopyroxene and plagioclase. J Metamorph Geol 16:729–748
Zeilinger G (2002) Structural and geochronological study of the lowest Kohistan complex, Indus Kohistan region in Pakistan, NW Himalaya: Unpublished PhD, ETH Zurich
Zeitler PK (1985) Cooling history of the NW Himalaya, Pakistan. Tectonics 4:127–151